Neurotherapeutics (2022) 19:528–549
https://doi.org/10.1007/s13311-022-01217-8

ORIGINAL ARTICLE

Inter-alpha Inhibitor Proteins Ameliorate Brain Injury and Improve Behavioral Outcomes in a Sex-Dependent Manner After Exposure to Neonatal Hypoxia Ischemia in Newborn and Young Adult Rats

Xiaodi Chen[1] · Jiyong Zhang[1] · Yuqi Wu[1] · Richard Tucker[1] · Grayson L. Baird[2] · Rose Domonoske[1] · Adriel Barrios-Anderson[1] · Yow-Pin Lim[3,4] · Kevin Bath[5,6] · Edward G. Walsh[7] · Barbara S. Stonestreet[1]

Accepted: 7 March 2022 / Published online: 15 March 2022

Abstract

Hypoxic-ischemic (HI) brain injury is a major contributor to neurodevelopmental morbidities. Inter-alpha inhibitor proteins (IAIPs) have neuroprotective effects on HI-related brain injury in neonatal rats. However, the effects of treatment with IAIPs on sequential behavioral, MRI, and histopathological abnormalities in the young adult brain after treatment with IAIPs in neonates remain to be determined. The objective of this study was to examine the neuroprotective effects of IAIPs at different neurodevelopmental stages from newborn to young adults after exposure of neonates to HI injury. IAIPs were given as 11-sequential 30-mg/kg doses to postnatal (P) day 7–21 rats after right common carotid artery ligation and exposure to 90 min of 8% oxygen. The resulting brain edema and injury were examined by T_2-weighted magnetic resonance imaging (MRI) and cresyl violet staining, respectively. The mean T_2 values of the ipsilateral hemisphere from MRI slices 6 to 10 were reduced in IAIP-treated HI males + females on P8, P9, and P10 and females on P8, P9, P10, and P14. IAIP treatment reduced hemispheric volume atrophy by 44.5 ± 29.7% in adult male + female P42 rats and improved general locomotor abilities measured by the righting reflex over time at P7.5, P8, and P9 in males + females and males and muscle strength/endurance measured by wire hang on P16 in males + females and females. IAIPs provided beneficial effects during the learning phase of the Morris water maze with females exhibiting beneficial effects. IAIPs confer neuroprotection from HI-related brain injury in neonates and even in adult rats and beneficial MRI and behavioral benefits in a sex-dependent manner.

Keywords Behavioral tests · Hemispheric tissue volume atrophy · Hypoxic-ischemic brain injury · Inter-alpha inhibitor proteins · Magnetic resonance imaging · Neuroprotection

Introduction

Neonatal hypoxic-ischemic (HI) brain injury that results in cerebral palsy (CP) and developmental delay are the most severe and common disabilities in childhood [1, 2]. CP is predominantly characterized by deficits in motor function and associated with a greater likelihood of having cognitive impairment after exposure to severe HI injury [3, 4]. Hypothermia, the only approved therapy for hypoxic-ischemic encephalopathy (HIE) in infants, unfortunately, is only partially protective [5–7]. It has a relatively narrow time

Xiaodi Chen and Jiyong Zhang are equal first author contributions

✉ Barbara S. Stonestreet
bstonestreet@wihri.org

[1] Department of Pediatrics, Infants Hospital of Rhode Island, Warren Alpert Medical School of Brown University, Women &101 Dudley Street, Providence, RI 02905-2499, USA

[2] Department of Diagnostic Imaging, Biostatistics Core Lifespan Hospital System, Rhode Island Hospital, Warren Alpert Medical School of Brown University, Providence, RI, USA

[3] ProThera Biologics, Inc, Providence, RI, USA

[4] Department of Pathology and Laboratory Medicine, Warren Alpert Medical School of Brown University, Providence, RI, USA

[5] Division of Developmental Neuroscience, New York State Psychiatric Institute, New York, NY, USA

[6] Department of Psychiatry, Columbia University Irving Medical College, New York, NY, USA

[7] Department of Neuroscience, Brown University, Providence, RI, USA

window up to 6 h after birth, during which hypothermia is most efficacious, and can only be used to treat full-term infants [8–12]. There is no therapy other than supportive care to "treat" or prevent brain damage in premature infants. Therefore, adjunctive treatment strategies, which target short- and long-term neuropathological damage along with motor and cognitive deficits, are critically needed for neonates that have been exposed to HI.

Selective targeting of early indicators of HI brain injury such as apoptotic/necrotic cell death, oxidative stress, and mitochondrial dysfunction [13, 14] has not yielded effective neuroprotective strategies most likely because these injuries are not reversible [15]. However, accumulating evidence suggests that modulating immune-mediated inflammation, which contributes to the development of delayed injury in HI [16], could be an efficacious neuroprotective strategy [17–19].

Inter-alpha inhibitor proteins (IAIPs), which are a family of structurally related anti-inflammatory immunomodulatory proteins, have received increasing attention due to their contribution to many disease states including HI-related brain injury in newborn and stroke in adult subjects [20–22]. The major forms of IAIPs found in human plasma are inter-alpha inhibitor (*IaI*), consisting of two heavy chains and a single light chain, and pre-alpha inhibitor (*PaI*), consisting of one heavy chain and one light chain [23, 24]. The light chain is also known as bikunin, which includes two protease inhibitor domains and functions as a serine protease inhibitor [24]. The heavy chains stabilize and construct extracellular matrix tissues and synergize with the activity of bikunin [23]. Previous work suggests that bikunin has neuroprotective properties such as reducing the size of stroke-related infarcts in adult rats [25], ameliorating brain damage in young pigs exposed to cardiopulmonary bypass [26], decreasing neuronal apoptosis in the hippocampus of adult gerbils after carotid artery occlusion [27], and increasing re-myelination in experimental autoimmune encephalitis in adult rats [28]. However, bikunin has a very short half-life (3–15 min) because of its renal clearance [29] when compared with the blood-derived complexes of IAIPs, which have a 23.1-h and 16.2-h half-life in neonatal HI-exposed male and female rats, respectively [30].

The blood-derived complexes of IAIPs inhibit destructive serine proteases, pro-inflammatory cytokines, and complement activation during systemic inflammation and improve survival after sepsis in neonates and adults [31–33]. In recent studies, we have shown that treatment of neonatal rodents with human plasma-derived IAIPs decreases neuronal cell death, reduces neuroinflammation, improves neuronal plasticity, and attenuates complex auditory processing deficits in neonatal male rodents after exposure to moderate HI [20, 21, 34–36]. They also attenuate lipopolysaccharide (LPS)–related disruption of the blood–brain barrier and reduce LPS-related increases in interleukin-6 in adult male mice [37]. In addition, IAIP treatment has been shown to improve histopathological outcomes including decreasing the quantity of infarcted brain tissue in both male and female neonatal rats after exposure to moderate and severe HI-related brain injury [21, 38].

However, our previous studies have mostly examined the short-term neuroprotective capacity of IAIPs to attenuate HI-related brain injury up to 10 postnatal (P) days in neonatal rats [21, 36, 38]. Our earlier studies only examined the effects of three doses of IAIPs given immediately, 24 and 48 h after exposure to HI. P10, 14, 20, 30, and 42 in rat pups are roughly equivalent to human term infants at full term (birth to 1 month), pre-weaning (6 months), toddler (2–3 years), pre-pubescent (8–9 years), and young adult (18 years) stages of brain development, respectively [39–42]. Although signs of HIE usually appear in the first few months, the neuropathologic processes of HIE continue to develop over time after the initial insult [43] and many children are diagnosed with CP at 2 years of age or later. Therefore, it is necessary to perform long-term follow-up at later developmental stages in patients with HIE. Furthermore, the pathological and behavioral outcomes after treatment with IAIPs on the progression of HI-related brain injury and the functional deficits over time have not been previously investigated.

Based upon the above considerations, the objective of the current study was to investigate sequential changes and later time points on neuropathological and behavioral effects of treatment with IAIPs in male and female rats exposed to HI brain injury as neonates. We hypothesized that systemic treatment with IAIPs has durable beneficial effects in the rat brain after exposure to HI injury as neonates, which is sustained throughout development. The Rice-Vannucci method was used to induce HI on P7 neonatal rats by exposure to right carotid artery ligation and 8% oxygen for 90 min. The brain of P7–10 rats is generally considered to be similar to the brain of near-term infants [39, 44, 45]. Although our earlier work demonstrated that systemic IAIPs have neuroprotective properties after HI in neonatal rats at the molecular, pathologic, and neurobehavioral levels [20, 21, 34–36, 38], this study is the first to administer repeated sequential doses of IAIPs for a total of eleven 30-mg/kg doses in an effort to examine the potential durable effects of IAIP administration after HI (Fig. 1).

Total body weight, growth rate, and brain weight were determined in the present study because they are known to be influenced by HI [38, 46, 47]. Brain injury and edema were determined by sequential measurements of magnetic resonance imaging (MRI) during the evolution of HI-related brain injury at P8, 9, 10, 14, 20, 30, and 41, along with hemispheric tissue volume atrophy at P42, respectively. Furthermore, a series of behavioral tests over 29 days from P7.5

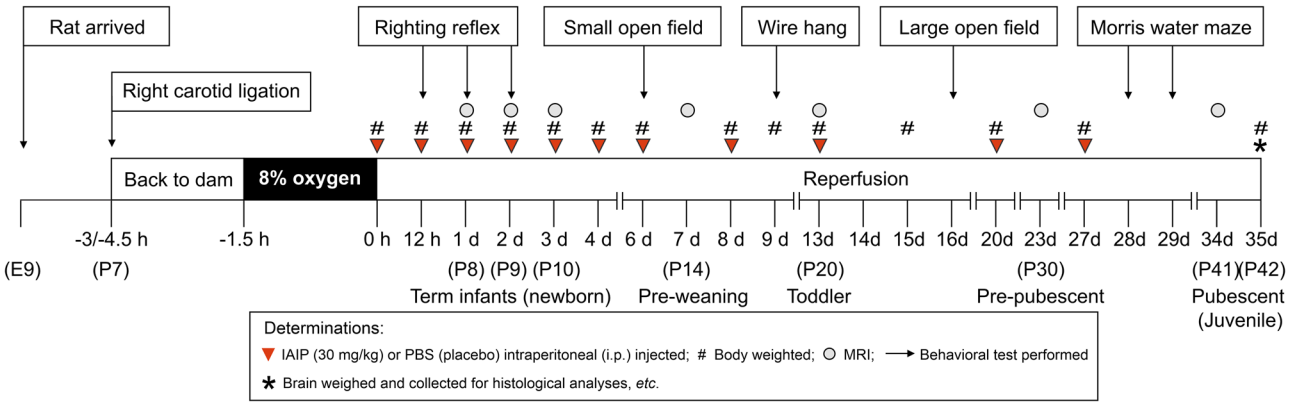

Fig. 1 Schematic diagram of the study design. The pups were returned to the dams for 1.5 to 3 h after right common carotid artery ligation. Thereafter, the pups were exposed to 8% oxygen with balanced nitrogen for 90 min at a constant temperature of 36 °C. Thirty mg/kg of human blood-derived IAIPs (inverted triangles) or an equal volume of placebo (PBS) were given intraperitoneally (i.p.) immediately (zero), 0.5, 1, 2, 3, 4, 6, 8, 13, 20, and 27 days after termination of hypoxia. Body weights (number signs) were measured at zero, 0.5, 1, 2, 3, 4, 6, 8, 9, 13, 15, 20, 27, and 35 days after hypoxia. The MRI scanning (gray circles) was performed at P8, P9, P10, P14, P20, P30, and P41. Cognitive and motor outcomes (arrows) such as righting reflex (P7.5, P8, P9), small open field (P13), wire hang (P16), large open field (P23), and Morris water maze (P35, P36) were examined. Thirty-five days after HI, a necropsy was performed, and the brain was collected for hemispheric tissue volume atrophy measurement (asterisk)

up to P36 in rats, which is roughly equivalent to the human brain development from full term infants up to young adult ages, were performed to examine the effects of treatment with IAIPs on the progression of HI-related motor and cognitive deficits over time.

Materials and Methods

The experimental procedures in this study were performed after obtaining approval from the Institutional Animal Care and Use Committees (IACUC) of Brown University and Women & Infants Hospital of Rhode Island. All experimental procedures were carried out following the National Institutes of Health (NIH) guide for the care and use of laboratory animals.

Preparation of IAIPs

IAIPs were produced and purified as previously described in detail [38, 48–50]. Briefly, high yield, pure (> 90%), and biologically active IAIPs were extracted from fresh frozen human plasma (Rhode Island Blood Center, RI, USA) by a scalable purification process with an anion-exchange chromatographic media (Toyopearl GigaCap Q650M, Tosoh Bioscience, King of Prussia, PA, USA) and an additional separation step with a proprietary synthetic chemical ligand affinity chromatographic media (Astrea Bioseparations, Cambridge, UK). The purity and biological activity of IAIPs were analyzed using sodium dodecyl sulfate polyacrylamide gel electrophoresis (SDS-PAGE), Western immunoblot, protein assay, and competitive immunoassay [20, 51]. Endotoxin in the purified products was monitored using a Limulus amebocyte lysate endotoxin-based chromogenic test (Pierce Biotechnology, Thermo Fisher Scientific, Waltham, MA, USA).

Animal Preparation and Surgical Procedures

Pregnant Wistar rats on embryonic day 15 (E15) or E16 were purchased from Charles River Laboratories (Wilmington, MA, USA) and housed in a 12-h light/dark cycled facility with ad libitum access to food and water in the Animal Care Facility at Brown University. The date upon which the rat pups were born was designated as P0. On P1, the pups were randomly culled to a maximum of 10 and balanced such that there were approximately equal numbers of males and females to reduce inter-litter variability. The pups were randomized as a block within each litter. Therefore, although an attempt was made to balance the sexes within the litters, this was not always feasible depending upon the number of males and females within the litters.

The Rice-Vannucci method was used to induce HI in neonatal rats [21, 52, 53]. On P7, the pups were randomly assigned to one of three groups: Sham-operated control (Sham), HI placebo-treated (HI-PL), or HI-IAIP-treated (HI-IAIP) groups. The pups were anesthetized with isoflurane (induction: 4%; maintenance: 2%) in oxygen and underwent right common carotid artery ligation, whereas the Sham animals were only exposed to a neck incision [52, 54]. After surgery, the pups were returned to their dams for 1.5–3 h for feeding and recovery. Then, the subjects exposed

to HI were placed in a temperature-controlled hypoxia (8% oxygen + 92% nitrogen) airtight chamber (BioSpherix, Parish, NY, USA) for 90 min. One non-ligated sentinel pup per litter had a rectal temperature probe placed (RET-4, Physitemp, Clifton, NJ, USA) to monitor body temperature. Rectal temperature was recorded every 10 min during HI and maintained close to 36.0 °C [7, 55]. Rectal temperature accurately reflects brain temperature after exposure to HI in rodents [56, 57]. The sentinel pup was not included in further investigations because the stress of the rectal probe placement alters the outcome of the HI studies [55, 58]. This HI model has been shown to result in approximately 60% unilateral brain injury 3 days after exposure to HI injury in our laboratory [21] similar to previous reports [59, 60]. The Sham subjects were placed in a similar chamber but exposed to room air. Only one pup died after surgery and HI with a mortality rate less than 3%.

Study Design

The study design is illustrated in Fig. 1. The HI-IAIP group received intraperitoneal (i.p.) injections with 30 mg/kg of IAIPs (ProThera Biologics, Inc., Providence, RI, USA) at zero, 0.5, 1, 2, 3, 4, 6, 8, 13, 20, and 27 days after completion of the exposure to HI (Fig. 1, inverted red triangles). The 30-mg/kg dose of IAIPs (first dose: zero h or 15 min after HI) was utilized because our previous studies have shown that the same dose of IAIPs ameliorated pathological brain injury, infarct volume, and neuroinflammation in neonatal rats 3 days after exposure to HI [21, 36]. The second dose of IAIPs was given 12 h after exposure to HI because the half-life of IAIPs with i.p. injections is 23.1 and 16.2 h following exposure to HI for males and females, respectively [30]. Sequential doses were administered in the current study because we sought to have a sustained effect of IAIPs over the course of these prolonged studies. The pups in the Sham-PL and HI-PL groups were given i.p. injections of equivalent volumes of phosphate-buffered saline (PBS) at the same time intervals.

The early dosing regimen was based upon our previous pharmacological findings [30]. The later dosing regimen (Fig. 1) was based upon our efforts to achieve sustained neuroprotective effects based the literature suggesting that HI and other insults early in life result in very prolonged effects on brain inflammation and in prolonged injury to the brain [61–65].

The neonatal rats were monitored and weighed at the time of each IAIP or PBS injection and also at 9, 15, and 35 days after HI (Fig. 1, number sign). The unilateral focal brain edema and injury formation were examined by MRI at P8, 9, 10, 14, 20, 30, and 41 (Fig. 1, gray circles). At each MRI analysis, 14 individual MRI predetermined brain slices were examined across the brain of each rat. In addition, behavioral tests including the righting reflex (P7.5, 8, and 9), small open field (P13), wire hang (P16), large open field (P23), and Morris water maze (P35 and P36) were performed (Fig. 1, arrows). On P42 (Fig. 1, star), the pups were sedated with a mixture of ketamine (74 mg/kg, i.p.) and xylazine (4 mg/kg, i.p.). The brains were perfused with PBS and 4% paraformaldehyde (PFA) via cardiac puncture at a flow rate of 3 mL/min. Thereafter, the brains were removed, weighed, post-fixed in PFA for 24 h, and stored in 30% sucrose in phosphate buffer (0.1 M) at 4 °C before cryo-sectioning for hemispheric tissue volume atrophy analysis [21, 66].

MRI Protocols

All MRI image findings were obtained using a 3.0 Tesla Siemens Prisma scanner (Siemens Medical Solutions, Malvern, PA, USA) at the Brown Magnetic Resonance Facility. A Siemens 16 channel hand/wrist array was used for signal reception with the two-channel body coil used for transmitting. Anesthesia was delivered using a manifold splitter that allowed for simultaneous scanning of up to four rats. Anesthesia consisted of isoflurane in oxygen at 4% for induction and 1–2% for maintenance during scanning. Each animal was placed on a holder with an integral nosecone for gas delivery. Once the animals were placed in the array, a circulating water warming blanket was placed over the array to maintain body temperature. Scanning was performed at P8, 9, 10, 14, 20, 30, and 41. Four animals were scanned simultaneously up to P20. Three animals were scanned simultaneously at P30 because of increases in growth and two scanned simultaneously at P41. Animals were aligned such that the brains of all animals could be captured with a single multi-slice acquisition.

After placement into the imaging position of the scanner, a set of gradient-echo scout images were obtained. The slice stack position was determined for the acquisition of T_1-weighted anatomic reference images from the scouts and multi-echo T_2-weighted spin-echo scans for T_2 mapping. The anatomic reference data was obtained using an inversion recovery T_1-weighted 3D rapid gradient-echo sequence with a field of view of 129 mm and a reconstruction matrix of $256 \times 256 \times 224$ giving 0.5-mm in-plane resolution and slice thickness with 14 slices providing coverage from the frontal to the occipital brain. Timing parameters were repetition time = 2700 ms, inversion time = 952 ms, and echo time = 2.96 ms. Read flip angle was 9 degrees. Scan time was 6 min 33 s. T_2 data was obtained using a multi-slice 2D spin-echo acquisition with a field of view = 112 mm and in-plane reconstruction matrix = 256×256 giving a voxel size of 0.44 mm with 1-mm slice thickness. Repetition time was 2500 ms with echo times of 12.8–153.6 ms in 12.8-ms steps (12 echoes). Scan time was 8 min 27 s. No signal averaging was used for either the anatomic reference or spin-echo scans.

T_2 maps were computed on a pixel basis using a three-parameter nonlinear least-squares fit of signal intensity versus echo time using the expression:

$$S(TE) = S_0 e^{-TE/T_2} + DC$$

where *S(TE)* is the pixel intensity at echo time TE, S_0 is the equilibrium signal, *TE* is the echo time, T_2 is the calculated T_2 value, and *DC* is the offset (noise floor). The intensities (T_2 values) were averaged over the entire hemispheres to reduce possible subjectivity. Maps were computed using a MATLAB script (MathWorks, Inc., Natick, MA, USA), which read the scanner DICOM data and performed the least-squares fitting.

The extent of the injury was defined based on T_2 maps using 150 ms as the threshold for establishing edema [67–70]. Injury regions were included within manually drawn regions of interest intended to reject the ventricles (CSF has T_2 values close to that of pure water and would show as injury). Pixels in each slice were automatically counted and multiplied by the size of the volume element (0.1936 mm^3) to give the injury volume for a given slice. Injury volumes for all slices were then summed to give the total hemisphere injury volume. Identification of pixels corresponding to injury was performed using a MATLAB (MathWorks, Inc.) script based on the 150-ms threshold. All MRI images were analyzed by an examiner who did not have knowledge of the study group assignments.

Hemispheric Tissue Volume Atrophy Measurements

To measure the hemispheric tissue volume atrophy after exposure to HI, the brains were cut into four or five 2-mm coronal sections using a brain slicer matrix (Zivic Instruments, Pittsburgh, PA, USA), immersed in Tissue-Tek optimal cutting temperature (OCT) compound (Sakura Finetek, Torrance, CA, USA), and frozen in a metal beaker containing isopentane (MilliporeSigma, Burlington, MA, USA) surrounded by crushed dry ice [21, 38, 66]. Five cryosections (20 µm) were obtained from each 2-mm section and mounted on gelatin coated Superfrost™ Plus microscope slides (Fisher Scientific International, Inc., Hampton, NH, USA). Every third cryosection (20 µm) was randomly selected to be stained with cresyl violet (MilliporeSigma) for evaluation of HI cell injury [21, 38, 66]. The images of the cresyl violet–stained brain sections were obtained using a Micropublisher 6 CCD Camera (Qimaging, Surrey, British Columbia, Canada) to quantify the hemispheric tissue volume atrophy of the whole hemispheres and damaged areas of the brains in the study groups. The resultant images were analyzed with ImageJ (NIH, Bethesda, MD, USA) by an examiner who did not have knowledge of the study group assignments. The tissue area atrophy was calculated as a percent of the damaged hemisphere to the total contralateral hemisphere with correction for hemispheric edema, according to the following formula: tissue area atrophy (%) = [1 − (total ipsilateral hemisphere − ipsilateral hemisphere damage)/total contralateral hemisphere)] × 100% [21, 38, 46, 71, 72]. The respective volumes were calculated from each measured area by multiplying the distance (2 mm) between the sections. The values calculated by the two examiners were averaged and used in the final data analysis.

Behavioral Analyses

Rats were brought to the testing area and allowed to acclimate for a minimum of 15 min before beginning the behavioral procedures. All behavioral tests were digitally recorded with a monochrome GigE camera (Noldus, Leesburg, VA, USA) and analyzed without knowledge of the treatment group.

Righting Reflex Test

On P7.5, P8, and P9, the test was performed to track potential improvement in early motor coordination following exposure to HI. Briefly, the rat was placed in a supine position on a flat surface, and the latency to right itself to a prone position (all 4 paws in contact with the surface) was measured in seconds. Analysis of the reciprocal of seconds (1/s) was determined. The test was repeated for 5 consecutive trials.

Small and Large Open Field Tests

A single rat was placed in the center of a small empty arena (38.1 cm × 61.0 cm) on P13 for the small open field test and allowed to freely explore the field for 5 min. Similarly, a single rat was placed in the center of a large open field (43.2 cm × 86.4 cm) on P23 and allowed to freely explore the field for 10 min. The behavior of the rat was tracked from video files using EthoVision software (Noldus). Dependent measures included total distance traveled (cm). These tests were repeated on 3 consecutive trials and assessed basal motor activity and exploratory behaviors during early life.

Wire Hang Test

The rat was allowed to grasp onto a wire mesh cage top at P16. The cage top was then slowly inverted 180 degrees and the latency (sec) to fall was measured for 5 consecutive trials. The dependent measure included the maximum time to fall and provided an indication of sensorimotor function and muscular endurance in young animals after exposure to HI.

Morris Water Maze Test

Spatial memory and learning were determined by the Morris water maze tests in accordance with previously published protocols [73, 74] with modifications as follows. The tasks included a training phase on day 1 (P35) and a retrieval phase on day 2 (P36). On day 1 (P35), a circular pool (150 cm in diameter, Noldus) was filled with clean colored water (25 ± 1 °C) and virtually divided into four quadrants: north (N), south (S), east (E), and west (W). A platform (14 cm × 14 cm) was placed in the center of the S quadrant and rendered invisible as it was located approximately 2 cm below the surface of the colored water. The rat was first gently lowered into the pool from one fixed point (initial start position) in the N quadrant, facing the wall, and required to swim until the platform was located. The rat was allowed 10–20 s to rest after locating the platform. If the rat was not able to locate the platform within 2 min, the rat would then be guided gently toward the platform. The process was repeated for 5 additional trials with the identical start position for each trial. The objective of this task was to establish the learning curve for the rats after exposure to HI-related brain injury with and without treatment with IAIPs.

Three independent trials were performed on day 2 of the water maze tests (P36). Trial 1 was conducted exactly as on the first day. The latency (s) to find the hidden platform was recorded with tracking EthoVision software (Noldus). If the rat was not able to find the platform within 2 min, the rat was guided to the platform and permitted a short rest period (10–20 s). After completion of trial 1, in order to ascertain that the rat was aware of the location of the hidden platform, a second trial (a spatial probe trial) was performed as follows: the hidden platform was removed, and then the rat was placed at the start position of the pool for a total of 2 min. The purpose of trial 2 was to test the ability of the rat to approximate the location of the platform, which was determined by how quickly the rat reached the quadrant where the hidden platform had been (S quadrant) as well as the time spent swimming in the proximity to the location of the previously hidden platform. The percent of the time that the rat spent in the S quadrant was calculated as follows: time spent in the S quadrant divided by trial length (2 min). The platform was returned to the same designated position for trial 3, except the platform was now visible to the rat because it was raised to approximately 1 cm above the water surface. This trial was to ensure that differences in latency to localize the platform were due to spatial abilities and not because of impaired ability to swim. The test was performed and the time to reach the platform was recorded as in trial 1.

Statistical Analyses

Body weight gain between treatment groups was compared across time points by a two-factor analysis of variance (ANOVA) for repeated measures. The results of the brain weight and the hemispheric tissue volume atrophy were first tested for a single outlier using Grubb's test (two-sided) [75, 76] or outliers from nonlinear regression using the ROUT test [77] (GraphPad Prism, San Diego, CA, USA). Then, the data distribution was tested using the Shapiro–Wilk normality test. ANOVA was used for normally distributed data and the Kruskal–Wallis test used for data that was not normally distributed. The results from the hemispheric tissue volume atrophy measurements were analyzed with Kruskal–Wallis test followed by Dwass, Steel, Critchlow-Fligner Multiple Comparisons Test as a post hoc test. The differences in sex and the interactive effects of multiple categorical independent variables in body and brain weights (sex versus treatment) and hemispheric tissue volume atrophy (sex versus treatment) over time were analyzed with factorial ANOVA. If a significant difference was detected by ANOVA, Tukey's honestly significant difference (HSD) test for multiple comparisons was used as a post hoc test. The results of body weight, brain weight, and hemispheric tissue volume atrophy measures were expressed as mean ± standard deviation (SD).

The MRI results were analyzed using SAS Software 9.4 (SAS Inc, Cary, NC, USA). All modeling was accomplished with the GLIMMIX procedure. The mean T_2 values (ms) of the right and left hemispheres were modeled over time and by the slice between treatment conditions and between males and females using generalized mixed modeling (GLMM) with sandwich estimation assuming a log normal distribution, where observations were nested within rats. Planned comparisons between treatment conditions were compared between slices 6–10, where the most edema formed and were matched to the parietal cortex. Alpha was established at the 0.05 level, and all interval estimates were calculated for 95% confidence (CI). The Spearman rank-order correlation was used to compare the ratio of mean T_2 values of the right hemisphere to the left hemisphere (P41) and the hemispheric tissue volume atrophy (P42).

SAS Proc mixed linear modeling was used for the behavioral analyses with the group, time, sex, and group × sex interaction used for regression analyses of the righting reflex, wire hang, and small and large open field tests. The results were expressed as mean ± SD. The data for the righting reflex were analyzed as reciprocal of seconds and the data for small open field was log-transformed because of non-normal distributions. The Cox proportional hazard regression model with time-to-event as the outcome and with the group, time, sex, and group by sex interactions as independent variables

was used for the Morris water maze analysis [78]. Group differences were determined with least-squares means, and the results were expressed as median ± interquartile range. All statistical analyses were performed using the STATISTICA package (TIBCO Software Inc., Palo Alto, CA, USA), with the exception of the outlier analysis (GraphPad Software Inc.), and hemispheric tissue volume atrophy and MRI and behavioral analysis, which used SAS (Version 9.4, SAS Institute). $P < 0.05$ was considered statistically significant.

Results

Body Weight Gain and Brain Weight Changes After IAIPs or Placebo Treatment in Neonatal Rats Exposed to HI

Figure 2A summarizes the body weight gain changes after HI-related brain injury plotted as a percent (%) for the total group of males and females (males + females) and separately for the males and females in the Sham, HI-PL, and HI-IAIP groups. Differences in body weight gain over time were observed between Sham, HI-PL, and HI-IAIP groups in the group of males + females (ANOVA, males + females: $F(2, 40) = 4.3328$, $n = 46$, $P = 0.0198$). The increase in body weight gain over time was greater in the Sham than that in the HI-PL (Tukey's HSD, males + females: $P = 0.0201$) group. Moreover, the body weight gain over time was also greater in the HI-IAIP than that in the HI-PL (Tukey's HSD, males + females: $P = 0.0047$) group. However, differences were not observed among the Sham, HI-PL, and HI-IAIP male subjects ($P = 0.2950$). The body weight gain over time differed significantly between the Sham, HI-PL, and HI-IAIP of female subjects (ANOVA, females: $F(2, 22) = 6.3416$, $n = 25$, $P = 0.0067$) and was greater in the Sham than that in the HI-PL, but not the HI-IAIP females (Tukey's HSD, females: $P = 0.0070$). Additionally, the total body weight at P42 was greater in the males + females of the HI-IAIP than in the HI-PL group suggesting that the improvement in weight gain was sustained for the duration of the studies (Fig. 2B, Tukey's HSD, females: $P = 0.0166$).

Figure 2C shows the total brain weights of the Sham, HI-PL, and HI-IAIP groups plotted for the combined group of males and females and separately for the males and females at the end of the study at P42. The brain weight differed between Sham, HI-PL, and HI-IAIP in the males + females (ANOVA, males + females: $F(2, 45) = 13.6860$, $n = 48$, $P < 0.001$). The brain weights were heavier in the Sham than those in HI-PL (Tukey's HSD, males + females: $P < 0.001$) group. Furthermore, the brain weights in the males + females at P42 (Tukey's HSD, males + females: $P = 0.0256$) were also heavier in the HI-IAIP than those in the HI-PL groups. The brain weights differed (ANOVA, males: $F(2, 19) = 4.4653$, $n = 22$, $P = 0.0257$) in the males among Sham, HI-PL, and HI-IAIP groups. The brain weights were heavier in the Sham compared to those of the HI-PL (Tukey's HSD, males: $P = 0.0250$) males. However, the brain weights did not differ (Tukey's HSD, males: $P = 0.6055$) between the HI-PL and HI-IAIP males. Also, the brain weights differed (ANOVA, females: $F(2, 23) = 9.2168$, $n = 26$, $P = 0.0012$) between Sham, HI-PL, and HI-IAIP groups in the females. The brain weights were heavier in the Sham compared to those from the HI-PL (Tukey's HSD, females: $P = 0.0009$) females. However, the brain weights did not differ (Tukey's HSD, females: $P = 0.1458$) between the HI-PL and HI-IAIP females. Moreover, although the brain to body weight ratio differed between the Sham, HI-PL, and HI-IAIP groups in the males + females (ANOVA, males + females: $F(2, 45) = 3.2723$, $n = 48$, $P = 0.0471$), the brain to body weight ratio did not differ in the males + females between the HI-PL and HI-IAIP groups (Supplementary Fig. 1). The brain to body weight ratio was also greater in the Sham than that in HI-IAIP (Tukey's HSD, males + females: $P = 0.0424$) group, but not in the HI-PL (Tukey's HSD, males + females: $P = 0.1102$) group. The ratio of brain to body weights did not differ between the Sham, HI-PL, and HI-IAIP groups in males ($P = 0.1306$) or females ($P = 0.2402$). Taken together these findings suggest that the weight gain was greater throughout the 42-day study in the HI-IAIP than that in the HI-PL males + females and that the systemic weight gain was associated with higher brain weight in the HI-IAIP than that in the HI-PL males + females. However, the higher brain weight could not be attributed to the heavier body weight because the brain weight as a percent of the body weight did not differ between the HI-IAIP and HI-PL males + females.

Treatment with IAIPs After HI Attenuated Edema Evolution and Formation in Female Neonatal Rats

Effects of IAIP treatment on brain edema/injury formation after HI was initially examined by T_2-weighted MRI at P8, P9, P10, P14, P20, P30, and P41 ages that are similar to human term infants, pre-weaning, toddler, pre-pubescent, and young adult developmental stages [39] (Fig. 1). Figure 3 shows the mean T_2 (ms) values for the total of the 14 scanned slices in both the left (systemic hypoxic exposed) and right (hypoxic-ischemic exposed) hemispheres. T_2 values changed as postnatal age increased differently between treatments and hemispheres by males + females and by male and female rats (SAS Proc GLIMMIX, $P < 0.0001$). Specifically, T_2 values for the Sham group decreased as postnatal age increased similarly across both hemispheres in the males + females and in the male and female rats. Likewise, T_2 in the HI-PL and HI-IAIP groups also decreased with postnatal age similarly to the Sham but only in the left hemisphere exposed to systemic

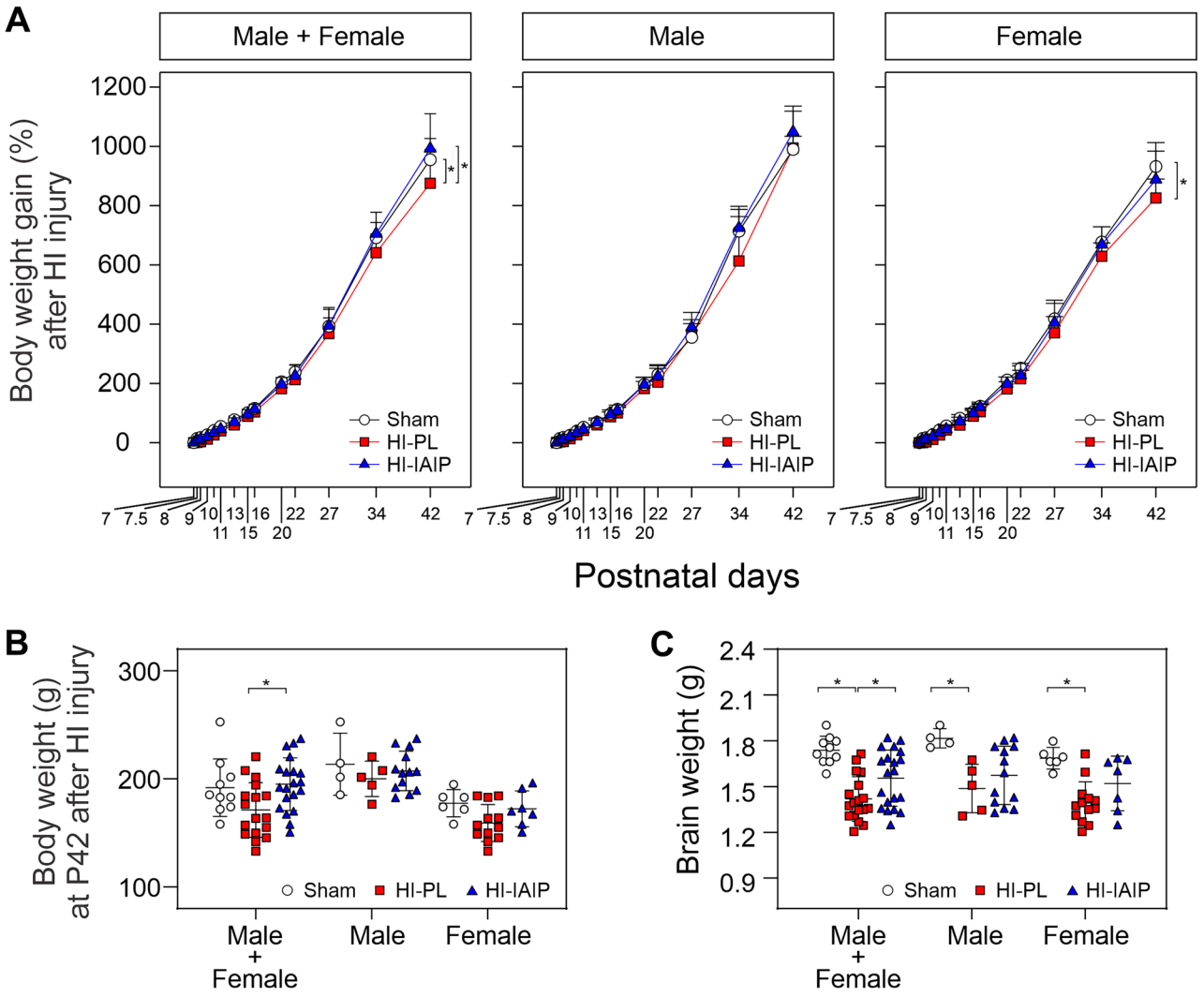

Fig. 2 Body weight gain overtime (%) and body and brain weight changes at P42 of the Sham (open circles), HI-PL (red squares), and HI-IAIP (blue triangles) groups. **A** Percent body weight gain on the y-axis plotted against study time in postnatal days on the x-axis for the total group of males + females, males, and females. Body weight gain (%) was lower in the HI-PL males + females compared to the Sham group during the study periods and greater in the HI-IAIP males + females compared to the HI-PL group during the studies. Body weight gain (%) did not differ between the Sham, HI-PL, and HI-IAIP males but was greater in the Sham compared to that from HI-PL females during the study periods. Sham: male $n=4$, female $n=6$; HI-PL: male $n=5$, female $n=12$; HI-IAIP: male $n=13$, female $n=7$. **B** Total body weight at P42 on the y-axis plotted for the males + females, males, and females on the x-axis. Body weight was higher in the HI-IAIP males + females compared to that of the HI-PL group. Body weight did not differ between the Sham, HI-PL, and HI-IAIP males and females. Sham: male $n=4$, female $n=6$; HI-PL: male $n=5$, female $n=12$; HI-IAIP: male $n=13$, female $n=7$. **C** Total brain weights (g) in the males + females, males, and females plotted as dot plots. Brain weights were lower in the HI-PL males + females, males, and females than those of the Sham group. Brain weights were higher in the HI-IAIP males + females compared to those of the HI-PL group, but not separately in the males or females. Sham: male $n=4$, female $n=6$; HI-PL: male $n=5$, female $n=13$; HI-IAIP: male $n=13$, female $n=7$. Values are mean ± SD. *$P<0.05$

hypoxia. In the right hemisphere exposed to HI-related brain injury, the T_2 values of HI-PL group were higher than those in the HI-IAIP group in both the males + females and female rats at P8, P9, and P10 (Fig. 3, asterisks, SAS Proc GLIMMIX, $P<0.05$) but not at P14, P20, P30, and P41, nor in the male rats (SAS Proc GLIMMIX, $P>0.05$), suggesting that treatment with IAIPs reduced HI-related brain edema formation and evolution early after exposure of the female rats to HI-related brain injury. The T_2 values in the HI-PL and HI-IAIP groups were higher than those in the Sham group in the males and females and males + females over entire study time periods (SAS Proc GLIMMIX, $P<0.05$).

We further investigated the mean T_2 values by slices in the right hemisphere, because differences in mean T_2 values were not detected between the study groups in the left hemisphere (Fig. 3, left, SAS Proc GLIMMIX, $P=0.9829$).

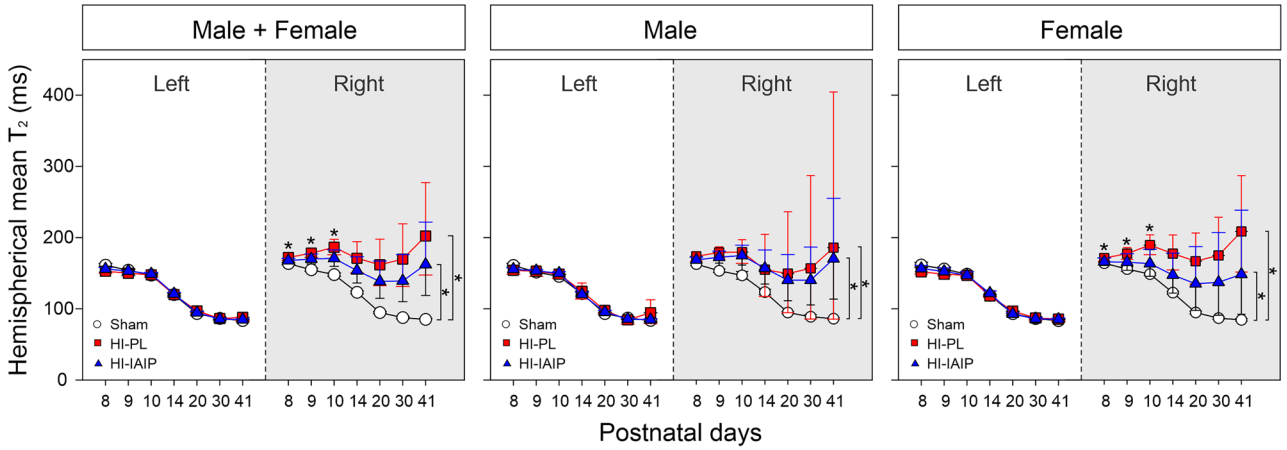

Fig. 3 The mean T_2 value (ms) of total 14-brain slices scanned by MRI at P8, P9, P10, P14, P20, P30, and P41 on left and right brain hemispheres. Sham (open circles), HI-PL (red squares), and HI-IAIP (blue triangles) groups. Decreases in mean Sham T_2 values were observed with increasing postnatal age across both left and right hemispheres for the males + females, males, and females, whereas changes in of T_2 were not observed between the Sham, HI-PL, and HI-IAIP groups in the left hemispheres. In the right hemisphere, the HI-PL values were higher (asterisks) than in the HI-IAIP group in the males + females and female rats at P8, P9, and P10. Sham: male $n=4$, female $n=6$; HI-PL: male $n=5$–7, female $n=13$; HI-IAIP: male $n=13$, female $n=7$. Values are mean ± 95% confidence interval (CI). *$P<0.05$ vs HI-PL

Furthermore, using the SAS GLIMMIX procedure, we analyzed the right brain sections from slices 6 to 10, because these sections represent the frontoparietal lobe, which is commonly damaged after HI-related insults [79]. The T_2 values for the males + females at P8 (SAS Proc GLIMMIX, $P=0.0381$), P9 (SAS Proc GLIMMIX, $P=0.0285$), and P10 (SAS Proc GLIMMIX, $P=0.0123$), but not P14, P20, P30, or P41 (SAS Proc GLIMMIX, $P>0.05$), were statistically higher in the HI-PL than those in the HI-IAIP groups (Fig. 4A, B). There were no significant differences in mean T_2 values (ms) between HI-PL and HI-IAIP groups in the males at P8, P9, P10, P14, P20, P30, or P41 (SAS Proc GLIMMIX, $P>0.05$). However, the T_2 values were lower in HI-IAIP females at P8 (SAS Proc GLIMMIX, $P=0.0225$), P9 (SAS Proc GLIMMIX, $P=0.0346$), P10 (Fig. 4A, SAS Proc GLIMMIX, $P=0.0104$), and P14 (SAS Proc GLIMMIX, $P=0.0444$), but not at P20, P30, or P40 (Fig. 4B, SAS Proc GLIMMIX, $P>0.05$) compared to the values of the HI-PL females. No significant treatment by sex interactions was observed (SAS Proc GLIMMIX, $P=0.8691$), whereas mean T_2 values between slice, treatments, sex, and time were statistically significant in the right hemisphere (SAS Proc GLIMMIX, $P<0.0001$).

Figure 5 shows representative T_2-weighted images demonstrating the effects of IAIPs on HI-related edema in brain slice 8 at P10. The hyperintense regions outlined by the yellow dashed lines were interpreted as edema. T_2-weighted imaging clearly showed edema covering the most of ipsilateral hemisphere in the HI-PL group in both the male and female in comparison with the Sham group. After IAIP treatment, the amount of the edema was reduced in the female but not in the male.

Treatment with IAIPs Reduces Ipsilateral Hemispheric Tissue Volume Loss at P42 in the Male + Female Rats After Exposure of Neonatal Rats to HI-Related Brain Injury

Figure 6A contains representative cresyl violet images of the coronal brain sections from the Sham, HI-PL, and HI-IAIP males (top row) and females (bottom row) rats at P42. Inspection of the coronal images reveals that the HI-PL group exhibited increased ipsilateral hemispheric pallor compared with the Sham group in both male and female rats. The HI-IAIP treated male and female rats did not appear to demonstrate major reductions in pallor compared with the HI-PL groups after exposure of the neonatal rats to HI-related brain injury.

Quantitative analysis of the percent hemispheric tissue atrophy confirmed the appearance of the cresyl violet–stained images in the neonatal rats exposed to HI after treatment with IAIPs (Fig. 6B). The hemispheric tissue volume atrophy was greater (64.5 ± 13.5%) in the HI-PL (Kruskal–Wallis, males + females: $P=0.0018$) compared with those of the Sham (7.8 ± 2.9%) group for the entire group of males + females. Treatment with IAIPs reduced (Kruskal–Wallis, males + females: $P=0.0410$) the hemispheric tissue volume atrophy to 35.8 ± 26.4% in the males + females. Therefore, treatment with IAIPs after exposure to HI reduced the hemispheric tissue volume atrophy by

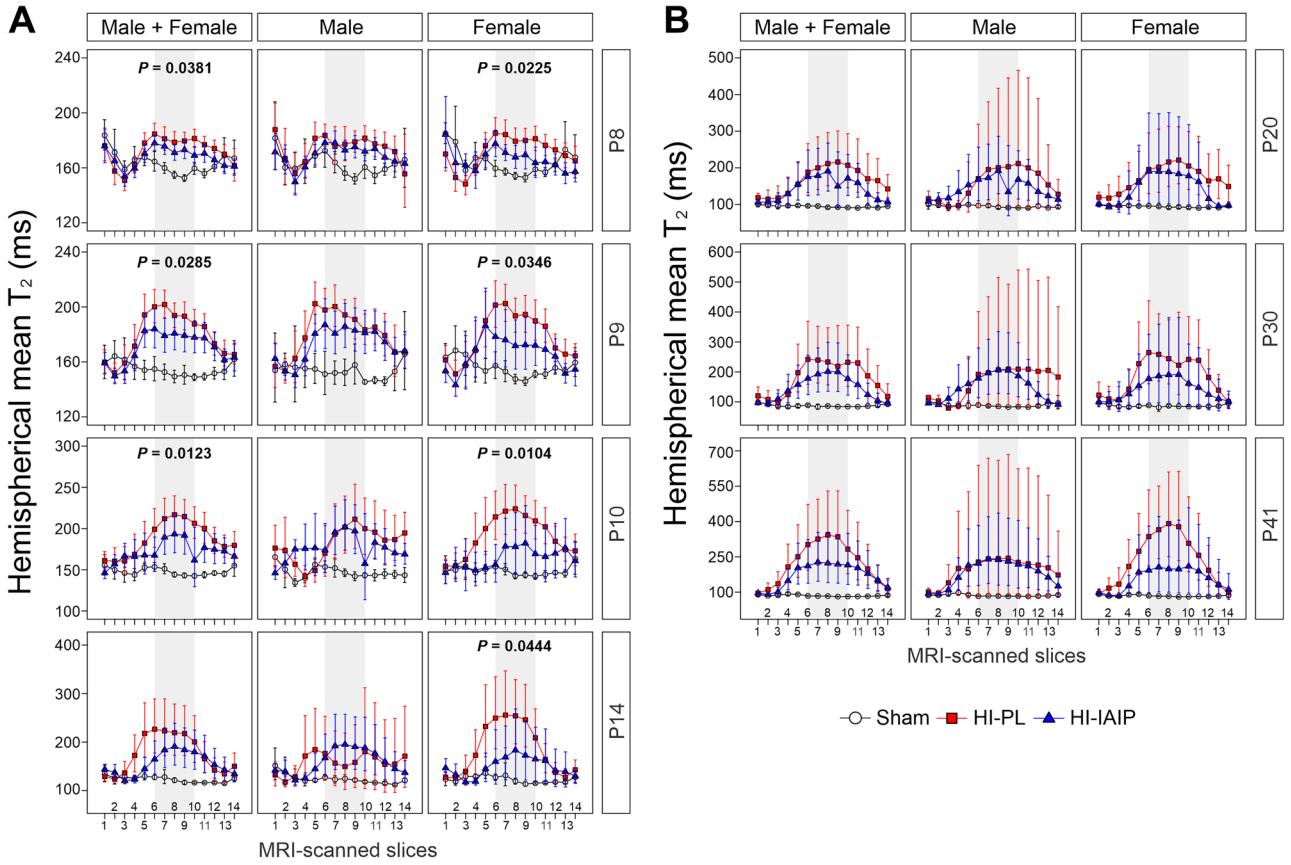

Fig. 4 The mean T2 values (ms) for the 14-brain slices scanned by MRI on P8, P9, P10, P14, P20, P30, and P41 in the right hemisphere. Sham (open circles), HI-PL (red squares), and HI-IAIP (blue triangles) groups. **A** The mean T_2 values from slices 6 to 10 (gray shaded areas) were lower in HI-IAIP males + females than in the HI-PL males + females at P8, P9, and P10, but not P14. The mean T_2 values from slices 6 to 10 (gray shaded areas) were lower in HI-IAIP than in the HI-PL females at P8, P9, P10, and P14. **B** Statistical differences were not observed between the mean T_2 values from slices 6 to 10 (gray shaded areas) in the study groups. Sham: male $n=4$, female $n=6$; HI-PL: male $n=5$–7, female $n=13$; HI-IAIP: male $n=13$, female $n=7$. Values are of mean ± 95% CI. Significant P values in bold (slices 6–10) on relevant panels

44.5 ± 29.7% in the total group of males + females. The hemispheric tissue atrophy was 69.5 ± 5.2% in the HI-PL males (Kruskal–Wallis, males: $P=0.0855$) and 8.7 ± 2.9% in the Sham males and was not reduced (Kruskal–Wallis, males: $P=0.0679$) by treatment with IAIPs. Similarly, the ipsilateral hemispheric tissue atrophy was 60.7 ± 17.4% in the HI-PL and 7.2 ± 3.0% in the Sham females (Kruskal–Wallis, females: $P=0.0284$), but the HI-related hemispheric tissue atrophy was not reduced (Kruskal–Wallis, females: $P=0.4385$) by treatment with IAIPs in the female subjects. Inspection of Fig. 6B suggests that the response of both the male and female rats to treatment with IAIPs was quite heterogeneous with some animals showing almost no injury and others showing injury that was in a similar range to those of the HI-PL groups (Fig. 6B, blue triangles). Although these findings could be interpreted to suggest that treatment with IAIPs in the total group of males and females reduces histopathological injury in rats after exposure of neonatal rats to HI-related brain injury, the separate findings in the males and females were not significant.

The Ratio of Right to Left T_2 MR Images at P41 Correlate with Hemispheric Tissue Volume Atrophy Measures at P42

The Spearman rank-order correlation was used to compare the MRI imaging scanned at P41 to the hemispheric tissue volume atrophy measured at P42 (Fig. 7). The MRI images were expressed as the ratio of T_2-weighted intensity in the right hemisphere (R, HI hemisphere) compared to the left (L, systemic hypoxic) hemisphere, whereas the hemispheric tissue volume atrophy was calculated as a percent ratio of the ipsilateral (right) hemisphere to the contralateral (left) hemisphere with correction for hemispheric edema. Significant correlations were observed in the total group of male + female ($R^2=0.4849$, $n=35$, $P<0.001$), male ($R^2=0.4559$, $n=20$, $P=0.0011$), and female ($R^2=0.4605$, $n=15$, $P=0,0054$) rats. These results support the contention that both MRI and hemispheric tissue atrophy analyses provide similar determinations of brain injury after exposure to

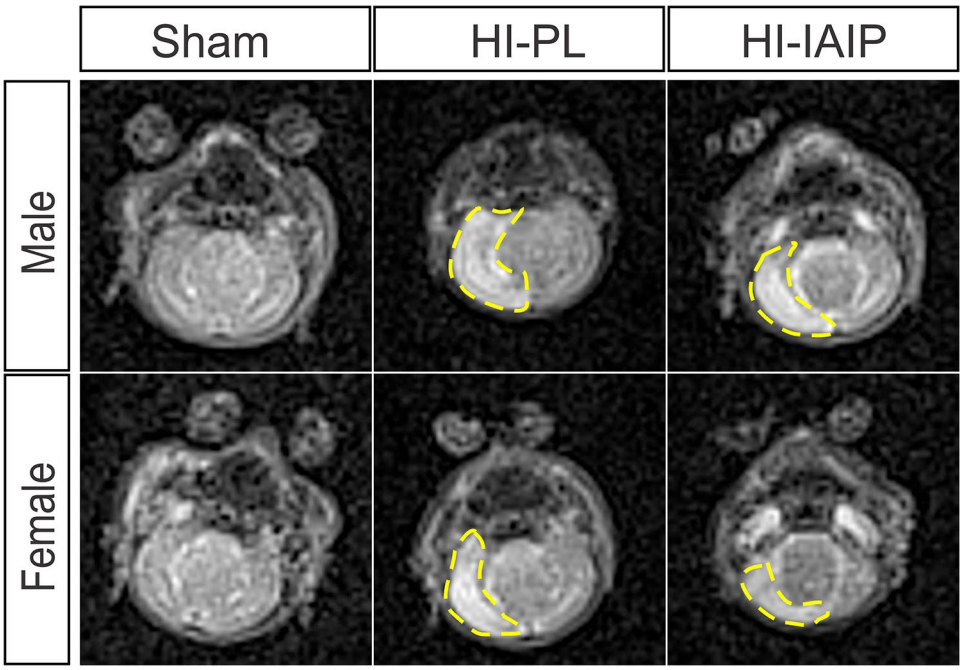

Fig. 5 Representative T_2-weighted images showing the HI-related brain edema/injury in the MRI-scanned slice 8 at P10. The hyperintense regions, which were interpreted as edema/injury, were outlined by yellow dashed lines. IAIP treatment reduced edema size in the female, but not in the male rat exposed to HI-related brain injury

HI in neonatal rats. In addition, it is important to emphasize that at the later stages after HI injury, T_2 is relatively high because of the presence of mainly fluid in the injured regions with limited amounts of particulate debris [80].

Treatment with IAIPs After HI Improved Short-Term Behavioral Performance in Male and Long-Term Behavioral Performance in Female Neonatal Rats

A battery of neurobehavioral tests was performed to examine the effects of treatment with IAIPs on HI-related short- and long-term functional outcomes (Figs. 8 and 9 and Supplementary Fig. 2). We first examined the effects of HI-related brain injury on the righting reflex to examine basic motor coordination skills during the early postnatal period in the neonatal rats 12, 24, and 48 h after the exposure to the HI insults (Fig. 8A). An analysis was first performed on the group of males + females to examine the effects of treatment on the combined group; the comparison was then followed up with separate analyses on the male and female subjects. The results of righting reflex (Fig. 8A) during the study periods (12, 24, and 48 h) are exhibited as the response latency time and represented as the reciprocal of seconds (1/s). There was a significant main effect of treatment in the males + females, with the HI-IAIP scoring significantly higher than the HI-PL group (SAS Proc mixed linear modeling, $P = 0.0265$). This effect of treatment with IAIPs was also present in the males (SAS Proc mixed linear modeling, $P = 0.0316$) but not in the females (SAS Proc mixed linear modeling, $P = 0.6704$). Supplementary Fig. 2 shows the results of righting reflex on each day of study. The treatment with IAIPs increased ($P = 0.0562$) the reciprocal response latency time (1/s) compared to placebo in the male + female (SAS Proc mixed linear modeling, $P = 0.0582$) group of HI-exposed rats on P8, but not on P7.5 or P9. Similarly, treatment with IAIPs increased reciprocal response latency time compared with placebo in the male (SAS Proc mixed linear modeling, $P = 0.0207$) neonatal rats that were exposed to HI on P8, but not on P7.5 or P9. However, differences in latency to right were not observed between HI-IAIP– and HI-PL–exposed females on P7.5, P8, or P9 (SAS Proc mixed linear modeling, all $P > 0.05$).

The small open field test was performed at P13 (preweaning period) to examine the effects of treatment with IAIPs on early general locomotive activity and exploratory behaviors in neonatal rats after exposure to HI-related brain injury. Compared to the Sham group, neonatal HI-related brain injury increased total distance traveled in the females (SAS Proc mixed linear modeling, $P = 0.0137$), but overall effects of treatment were not observed in the males + females or in the males (SAS Proc mixed linear modeling, $P > 0.05$, Fig. 8B). Differences between the HI-PL and HI-IAIP groups were not detected in total distance traveled (cm) in the overall analysis or in males and females alone (SAS Proc mixed linear modeling, all $P > 0.05$, Fig. 8B). There were no effects of sex (SAS Proc mixed linear modeling, all $P > 0.05$) for distance traveled, but a significant treatment vs sex interactions (SAS Proc mixed linear modeling, $P = 0.0219$) were detected.

On P16 (early postweaning period), we performed the wire hang test to evaluate both neuromuscular and locomotor

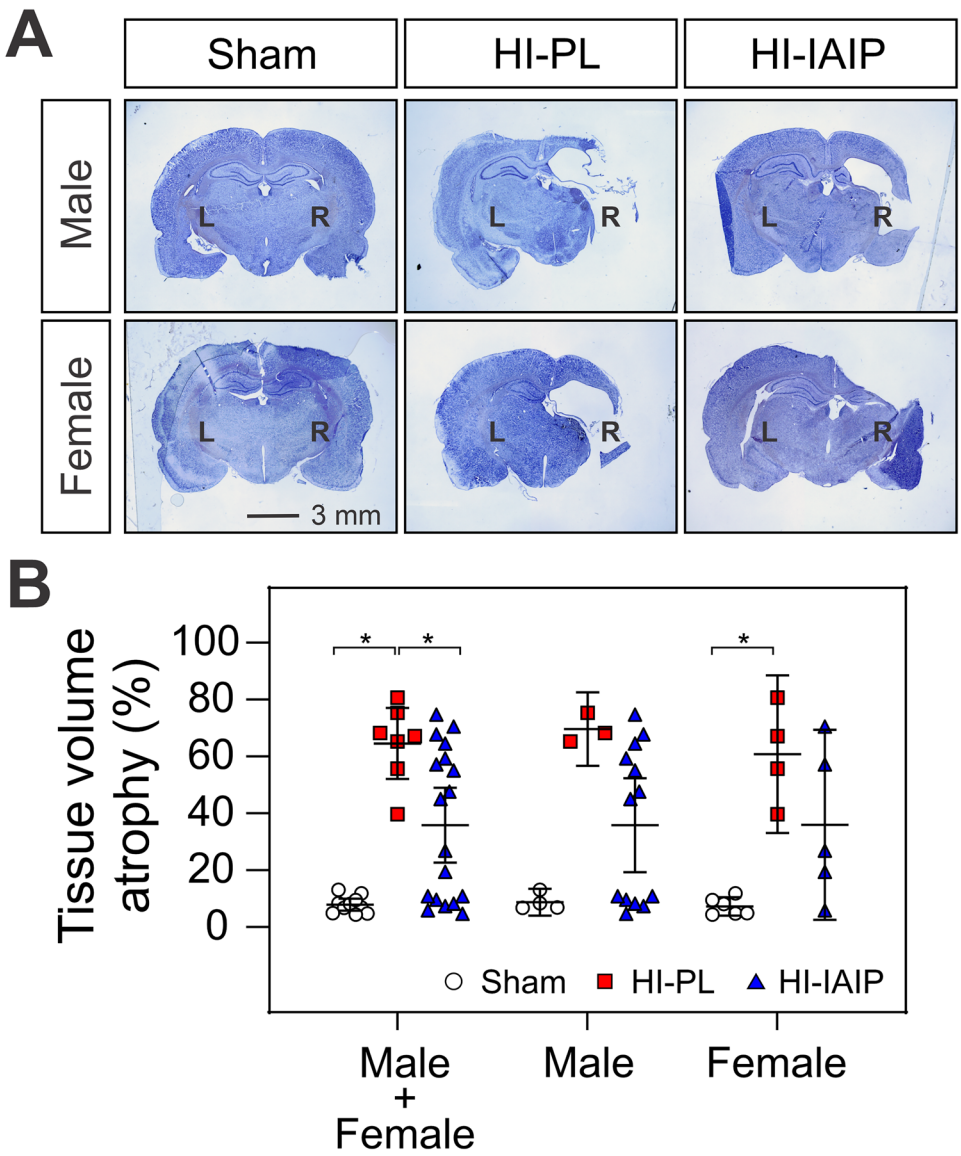

Fig. 6 Hemispheric tissue volume atrophy measurement after IAIP treatment. **A** Representative images of brain sections stained with cresyl violet 35 days after exposure to HI in the males (top row) and females (bottom row). Scale bar = 3 mm. **B** Percent hemispheric tissue volume atrophy plotted on the y-axis for the Sham (open circles), HI-PL (red squares), and HI-IAIP (blue triangles) groups on the x-axis for the males + females, males, and females. The hemispheric tissue volume atrophy was higher in the males + females of the HI-PL compared to the Sham and HI-IAIP groups. The hemispheric tissue volume atrophy was higher in HI-PL compared to the Sham group, but not in HI-IAIP females or males. Values are mean ± SD. *$P < 0.05$. Sham: male $n = 4$, female $n = 6$; HI-PL: male $n = 3$, female $n = 4$; HI-IAIP: male $n = 13$, female $n = 5$

function in neonatal rats exposed to HI with and without IAIP treatment. SAS Proc mixed linear modeling revealed that latency time (s) to fall from the wire was decreased in the HI-PL males + females (SAS Proc mixed linear modeling, $P = 0.0010$) and in the females (SAS Proc mixed linear modeling, $P = 0.0020$) compared to those in the Sham group. The latency to fall was increased (SAS Proc mixed linear modeling, $P = 0.0071$) in the HI-IAIP males + females and females compared with the HI-PL groups with this effect likely being driven by the significant effect in the treated females (SAS Proc mixed linear modeling, $P = 0.0046$) compared to the HI-PL rats (Fig. 8C). Differences were not observed between the Sham, HI-PL, and HI-IAIP groups of male rats (SAS Proc mixed linear modeling, $P = 0.5010$).

We also examined the long-term effects of treatment with IAIPs on motor function by examining the large open field test at P23 (early pre-pubescent period) to assess the late general locomotive activity and exploratory behaviors in rats after neonatal HI brain injury. No significant differences in total distance traveled (cm) were detected between the HI-PL and HI-IAIP groups in the overall analysis or in males or females separately (SAS Proc mixed linear modeling, all $P > 0.05$, data not shown). No main effect of sex and no treatment-related × sex interactions were observed (SAS Proc mixed linear modeling, all $P > 0.05$).

Long-term cognitive impairment can result from exposure to HI-related insults [81]. Therefore, we also performed the Morris water maze test to examine the long-term effects of treatment with IAIPs on spatial learning and memory at P35 and P36 rats (pubescent period) after neonatal HI brain injury. At P35 (day 1), using Cox's proportional hazards regression analysis, treatment with IAIPs decreased the mean

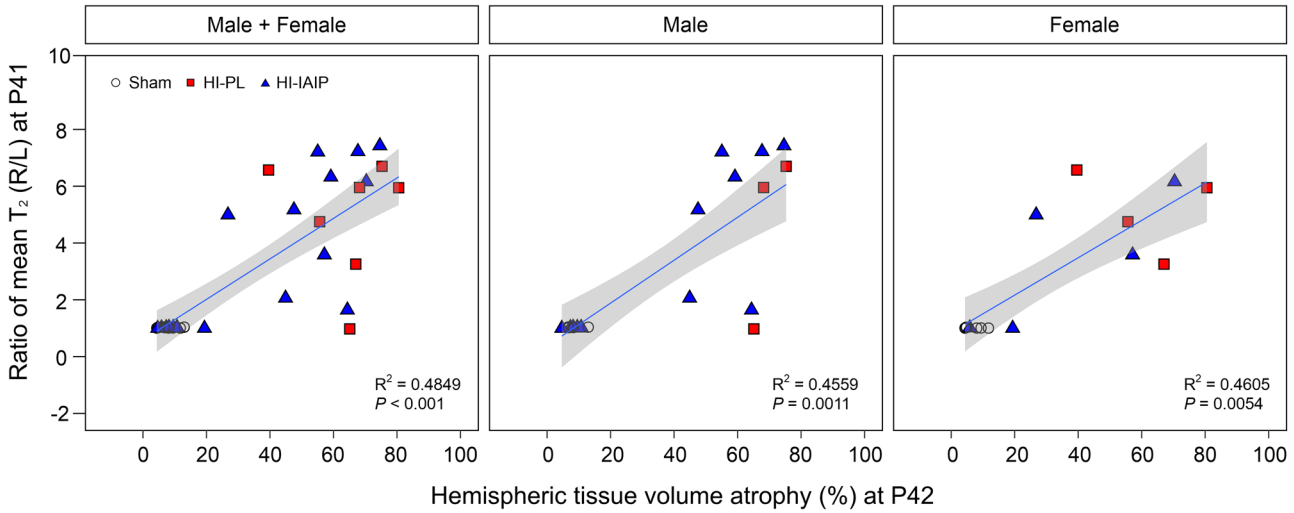

Fig. 7 Correlational analyses between T_2 MRI image analysis obtained on P41 and hemispheric tissue volume atrophy measured on P42. Sham (open circles), HI-PL (red squares), and HI-IAIP (blue triangles) groups. The ratio of mean T_2 values (ms) in the right hemisphere (R) to the left hemisphere (L) on the y-axis plotted against the hemispheric tissue volume atrophy as a ratio of the ipsilateral (R) hemisphere to the total contralateral (L) hemispheres with correction for hemispheric edema on the x-axis. Sham: male $n=4$, female $n=6$; HI-PL: male $n=3$, female $n=4$; HI-IAIP: male $n=13$, female $n=5$. The solid line designates the regression line. Gray shaded area is 95% CI. Statistical analysis by Spearman rank-order correlation

latency (s) to find the platform and led to improved performance in the HI-IAIP male + female group (hazard ratio HI-IAIP vs HI-PL = 1.6963, *CI* = 1.1386–2.5272, $P=0.0094$), with the effect being observed in HI-IAIP females (hazard ratio HI-IAIP vs HI-PL = 1.9012, *CI* = 1.0152–3.5607, $P=0.0448$) compared to HI-PL over the entire period of six trials. In the males, there was variability in performance on later trials, with no significant effect of treatment found for the day 1 performance (hazard ratio HI-IAIP vs HI-PL = 1.4517, *CI* = 0.8577–2.4570, $P=0.1650$, Fig. 9A). At P36 (day 2), no statistical differences were observed between HI-PL and HI-IAIP groups during trial 1 (latency measure), trial 2 (spatial probe trial measure), and trial 3 (latency measure) in the males + females or separately in the male and female rats (Fig. 9B, Cox's proportional hazards regression, all $P>0.05$). Furthermore, no main effects of sex or treatment × sex interactions were found at P35 or P36 (Cox's proportional hazards regression, all $P>0.05$).

The results of the neurobehavioral tests are schematically summarized in Fig. 10. The behavioral tests are listed on the specific postnatal days on which the test was performed, and the arrows compare the findings in the HI-IAIP and HI-PL groups. Treatment with IAIPs resulted in improved righting reflex from P7.5 to P9 in the males + females and in the males but not the females. Treatment with IAIPs did not affect the outcomes of the small open field on P13 or the large open field on P23. Treatment with IAIPs improved the results of the wire hang test at P16 in the males + females and females. Treatment with IAIPs improved the performance in the Morris water maze in the males + females and in the females during learning (P35), but not during the recall test (P36). Taken together, the results of the neurobehavioral tests suggest that treatment with IAIPs after exposure to HI in neonatal rats has significant protective effects in some but not all behavioral domains and that there is sex-related differential effects such that IAIPs have preferential effects for some tests in males and others in females.

Discussion

The primary objective of the current study was to determine whether treatment with human blood-derived IAIPs attenuates neuropathological brain injury characterized by MRI determined measures and the percent of total hemispheric tissue volume atrophy in young adult rats, along with behavioral outcomes during rodent development from neonates up to young adults after exposure of the neonates to HI. The study extends our previous work in which we have shown that treatment with IAIPs reduced neuronal cell death and brain infarct volumes within a relatively short time frame after treatment in P10 rats subsequent to exposure of P7 rats to HI [20, 21, 38]. In addition, we also have formerly shown that IAIPs improved juvenile non-spatial learning and adult spatial learning and working memory in rats after exposure of neonates to HI [20, 34, 35]. However, treatment with IAIPs in those studies was only given to male rats and administrated as a peri-insult paradigm prior to exposure to hypoxia [20, 34, 35]. Moreover, the effects of IAIPs on brain edema formation and evolution and locomotor deficits

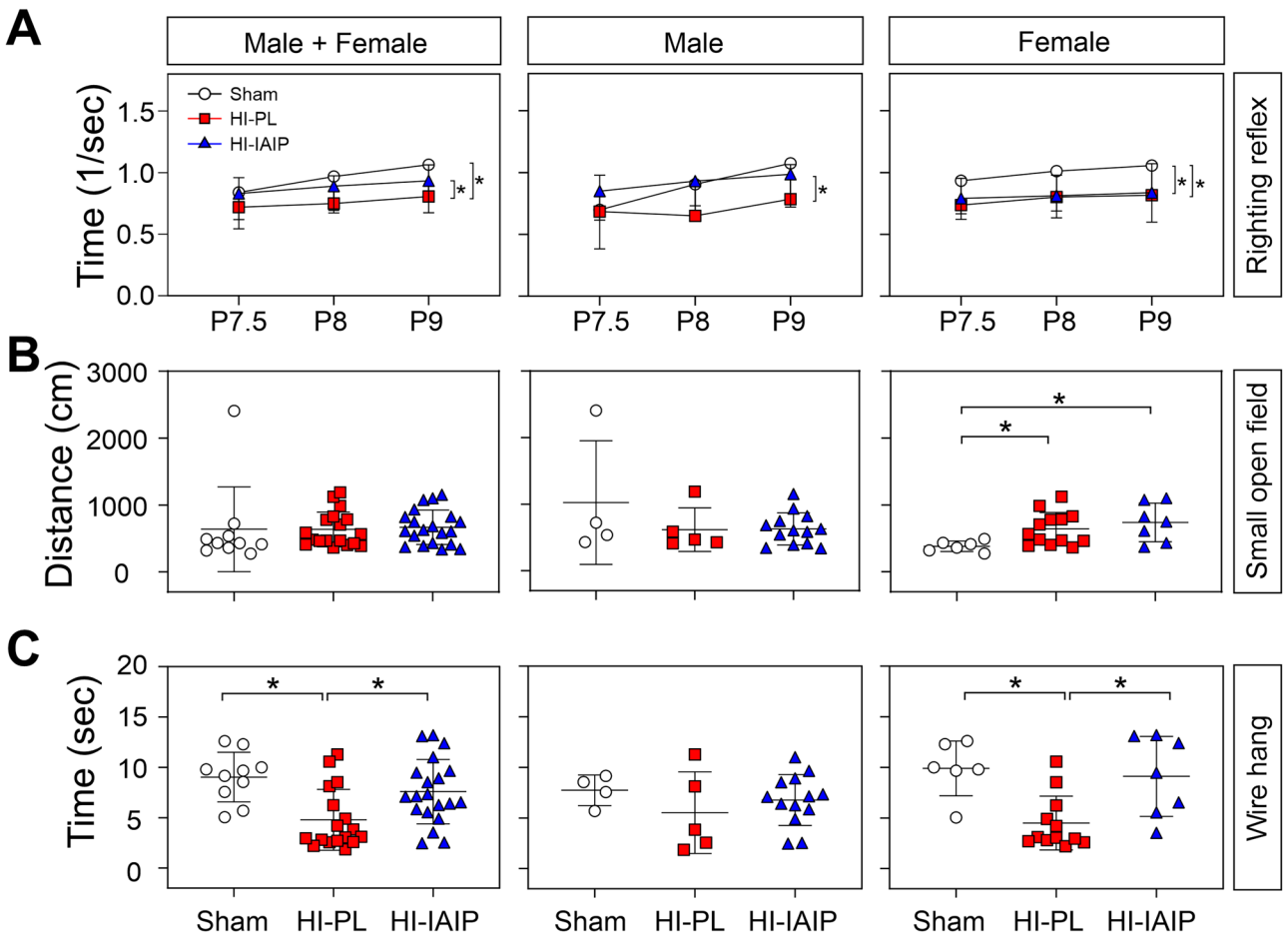

Fig. 8 The short-term effects of IAIP treatments on neurobehavioral outcomes in neonatal rats exposed to HI brain injury. Sham (open circles), HI-PL (red squares), and HI-IAIP (blue triangles) groups. **A** The general locomotor abilities over the study periods (P7.5, P8, and P9) were higher in the males + females and males in the HI-IAIP compared with the HI-PL group by the righting reflex test. The reciprocal response latency time (1/s) increased after treatment with IAIPs in the males + females and males compared to the HI-PL group, but not in the HI-PL females. Sham: male $n=4$, female $n=6$; HI-PL: male $n=7$, female $n=13$; HI-IAIP: male $n=13$, female $n=7$. (**B**) IAIP treatment did not affect the early general locomotive activity and exploratory behaviors in the small open field tests of the male + female, male, or female of the HI-PL groups. Sham: male $n=4$, female $n=6$; HI-PL: male $n=7$, female $n=13$; HI-IAIP: male $n=13$, female $n=7$. **C** Treatment with IAIP improved muscle strength/endurance by the wire hang test at P16 in the males + females and females compared to the HI-PL group, but not in the males. Sham: male $n=4$, female $n=6$; HI-PL: male $n=5$, female $n=12$; HI-IAIP: male $n=13$, female $n=7$. Values are mean ± SD. * $P<0.05$ vs HI-PL group. Statistical analysis by SAS Proc mixed linear modeling

were not examined in the previous reports. These are two common sequelae of HI-related brain injury during early development [82, 83].

In the current study, multiple doses of IAIPs were administered in an effort to maximize their efficacy over the prolonged time interval of the study and to demonstrate a durable effect in the young adult rats. The early treatment strategy was based on our previous work [21, 30, 36]. However, there was no information available to guide a strategy for long-term treatment with IAIPs. Therefore, we empirically elected to administer IAIPs during weeks 2–4 based upon the literature suggesting that early life HI and other insults result in very prolonged effects on brain inflammation and in prolonged injury to the brain. In fact, more recent information from studies in fetal sheep suggest that inflammation and injury is prolonged up to 1 to 3 weeks after an in utero insult [61, 62, 64, 65]. In addition, previous data in humans suggest that children with cerebral palsy have altered inflammatory responses even at school age [63]. Additionally, recent concepts indicate that there could be potential for late treatment after therapeutic hypothermia further to reduce inflammation and improve outcomes [61, 65]. Nonetheless, we cannot be certain that the IAIP treatment strategy that we have selected is the most optimal approach.

Given the above considerations, the overall goal of the current study was to extend our previous work by examining

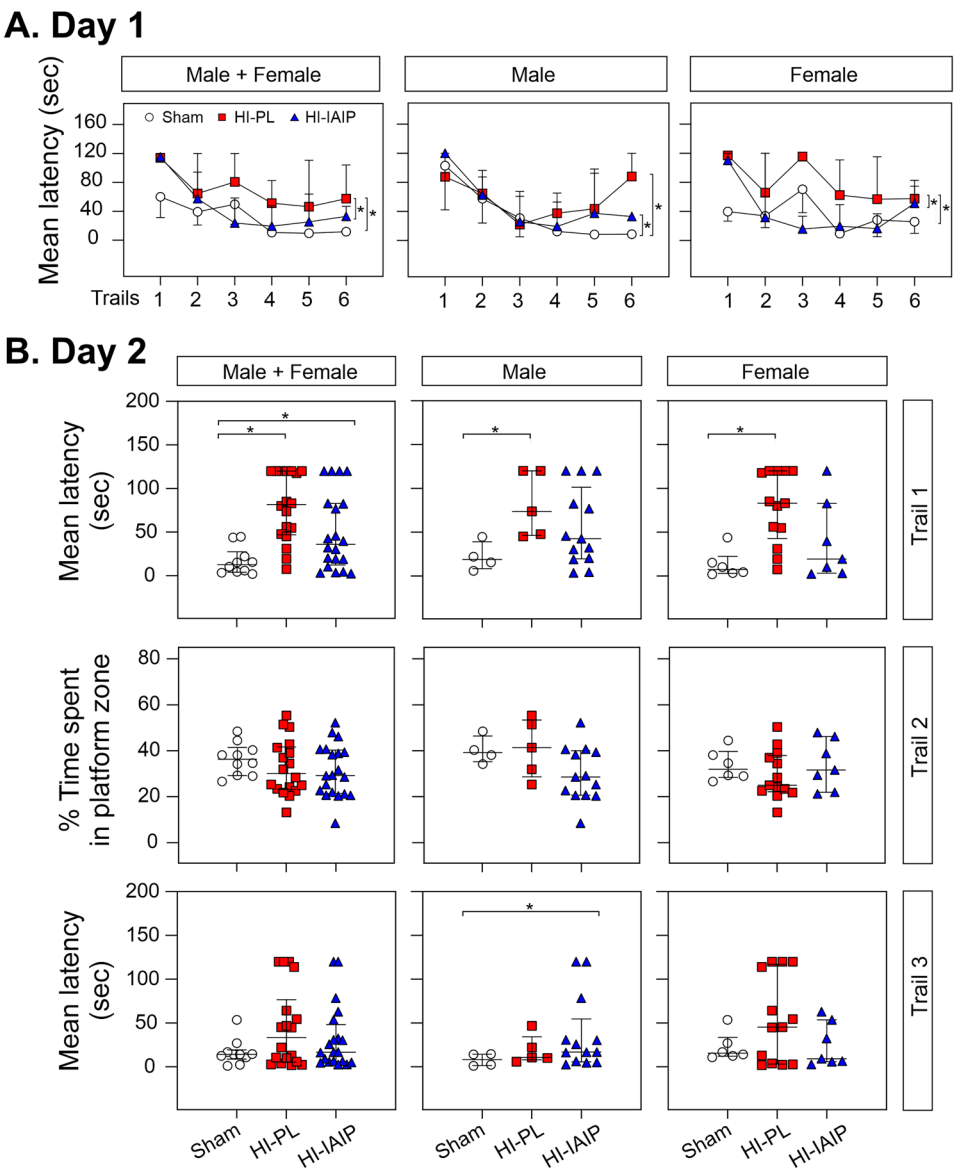

Fig. 9 Memory and learning assessment of the long-term effects of IAIPs on rats with neonatal HI brain injury using Morris water maze. Sham (open circles), HI-PL (red squares), and HI-IAIP (blue triangles) groups. **A** Treatment with IAIPs increased mean latency (s) in the males + females and females and had beneficial effects compared to the HI-PL group over the entire period of six trials at P35 (day 1), but not male rats. **B** On day 2 of the trial at P36, statistical differences between HI-IAIP and HI-PL groups were not detected in trials 1, 2, and 3 in the males + females, male, or female rats. Sham: male $n = 4$, female $n = 5$–6; HI-PL: male $n = 5$, female $n = 12$–13; HI-IAIP: male $n = 13$, female $n = 7$. Values are median ± interquartile range. * $P < 0.05$, statistical analysis by Cox's proportional hazards regression model

the effects of IAIPs during development from the neonatal to young adult ages on brain edema formation and evolution and locomotor deficits. The major findings of the current study are that systemic treatment with IAIPs after HI-related injury in neonates (1) improves body weight gain over time and attenuates HI-related reductions in brain weight in the entire group of young adult males and females rats (males + females); (2) reduces brain edema formation and evolution in the hemisphere ipsilateral to HI injury in the newborn and pre-weaning males + females and females; (3) attenuates brain hemispheric tissue volume atrophy in young adult rats; and (4) improves basic motor coordination abilities in the newborn male + female and male rats, and sensorimotor function and muscular endurance in the toddler-equivalent males + females and females, and spatial memory and learning in the young adult males + females and females. Consequently, treatment with IAIPs protects the brain from HI injury in neonates across neurodevelopmental stages in a sex-dependent fashion.

Previous work shows that HI-related insults impair somatic growth [84–86]. In the present study, we only observed HI-related reductions in body weight gain over time in the males + females and in the females (Fig. 2A), but not in the males, suggesting that body weight in young adult female rats was more sensitive to the impact of HI than that of the male rats. Our results are consistent with our previous findings showing that exposure to HI impaired short-term growth in both male and female neonatal rats [21, 38]. However, the current findings differ from a previous report showing that the growth rate in mice exposed to HI became more compromised as age was advanced and that males were more sensitive to the impact of HI than females after

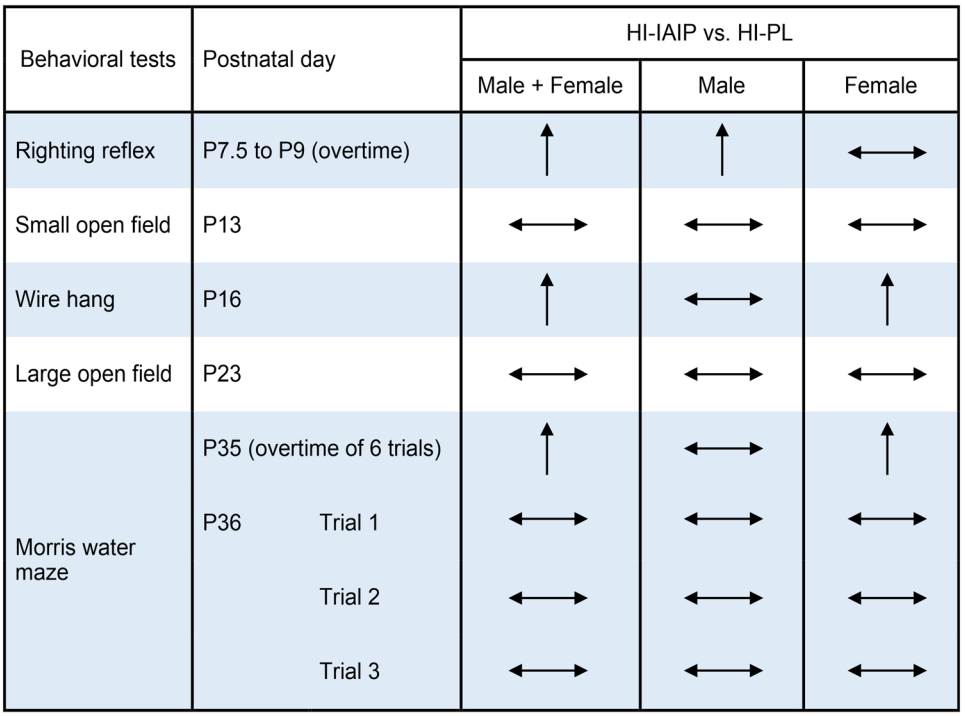

Fig. 10 Schematic summary of behavioral tests in the neonatal rats with and without exposure to IAIPs. ↑ indicates the improvement in behavior in the HI-IAIP compared with the HI-PL group. ↔ indicates no differences between the HI-IAIP and HI-PL groups

exposure of neonates to HI [87]. Nonetheless, weight was more impaired in young adults in both males and females [87]. Moreover, the trends in weight gain during the studies resulted in a lower total body weight in the total group of males and females that had been exposed to HI as neonates (Fig. 2B). In addition, treatment with IAIPs appeared to result in a higher total body weight at sacrifice (Fig. 2B). Combined with our previous findings suggesting that treatment with IAIPs improved body growth in neonatal male rats 3 days after HI injury [21, 38], our results suggest that treatment with IAIPs after exposure to HI as neonates could facilitate overall well-being such that the growth rate and resultant weight gain in young adults are improved by treatment with IAIPs. However, although the mechanism(s) by which IAIPs improved growth cannot be determined by the current study, the improved energy metabolism/balance and increased intake potentially play an important role [21, 38].

Treatment with IAIPs after exposure to HI in the neonates also appeared to exert beneficial effects on the brains of the young adults at P42 because the HI-related decreases in brain weight were attenuated by treatment with IAIPs (males + females, Fig. 2C). Brain weight is a reasonable measure of brain injury, because it correlates with morphometric changes after HI in neonatal rats and, therefore, is a representative indicator of overall brain damage [88]. The present findings are consistent with our previous report showing short-term brain weight sparing after treatment of male rats with IAIPs that were exposed to HI [21]. Consistent with the changes in absolute brain weight in the young adult rats, the HI-related changes in the MRI determined edema and/or injury formation and evolution (Figs. 3, 4 and 5), and brain hemispheric tissue volume atrophy (Fig. 6) was also attenuated by treatment with IAIPs.

In the current study, T_2-weighted MRI image analysis was used to examine brain tissue damage, edema formation, and evolution during rodent development in neonates from P8 up to P41 in young adult rats after exposure of P7 neonates to HI. Repeated scanning sessions were performed during development in the same rats over the periods covering major milestones during rodent brain development [39]. MRI has been considered as the most promising noninvasive tool to detect brain edema formation and evolution and injury in real time and the most effective method for detecting HI-related brain injury in neonates [89, 90]. A major strength of our study was that the MRI image analysis was performed in vivo during development in rats surviving HI as neonates rather than as terminal postmortem sample analysis [91, 92]. This was facilitated by the development of our specifically designed anesthetic manifold splitter that allowed for simultaneous repeated scanning of multiple rats over the course of development from P8 to P41.

T_2 decreases to a greater extent in white matter than in gray matter in the developing brain [93, 94]. There are at least two water compartments that contribute to the observed signal in white matter; these are the water contained within the myelin sheath (with short T_2) and the intra-axonal, intracellular, and the interstitial water (with longer T_2). Decreases

in T_2 values accompany the decreases in water concentration by two distinct mechanisms, one of which relates to changes in water compartmentalization [95], whereas the other mechanism involves increases in protein and lipid contents [96, 97]. The decreases in T_2 with development correspond to chemical changes in the myelin sheath [96, 98, 99]. Consistent with the known decreases in T_2 during development, which are associated with increases in white matter content, the measured T_2 values decreased in the Sham, HI-PL, and HI-IAIP groups on the hypoxic left side of the brain but only in the Sham group on the right side of the brain over the MRI scanning sessions (Figs. 3 and 4).

Although T_2 changes have been extensively examined during development and after exposure to HI in neonates [89, 91, 100–102], less information is available regarding the effects of therapeutic agents on changes in MRI image analysis after exposure to HI. In the current study, male and female rats were scanned for T_2 mapping changes in the brain at P8, P9, P10, P14, P20, P30, and P41 after exposure to HI at P7 with and without treatment with IAIPs (Fig. 4). Systemic treatment with IAIPs attenuated HI-related increases in the T_2 values in the ipsilateral parietal cortex at P8, P9, P10, and P14 in females and at P8, P9, and P10 in the males + females compared with those in the HI-PL group but did not affect the T_2 values after HI in the males. T_2-weighted MRI is considered a very reliable measure of injury in various neonatal rodent models [100, 103–106]. Therefore, our findings suggest that treatment with IAIPs attenuates the development of edema formation and evolution and/or injury relatively early after the exposure of neonatal rats to HI. In addition, we have shown a reasonably good correlation between injury measured by the ratio of right to left T_2 values at P41 and the histopathological hemispheric tissue volume atrophy at P42 (Fig. 7). Therefore, these findings suggest that treatment with IAIPs ameliorates the early effects of injury after HI, which may have important implications for the timing of treatment with IAIPs as alternative or adjunctive treatment to hypothermia for HIE.

Histopathological analysis is a standard method used to define tissue damage as an important end point of brain injury [107]. We have previously demonstrated that measurements of percent of infarct volume that account for the injury across the whole brain are more likely to exhibit superior sensitivity and accuracy and are more comprehensive than the semi-quantitative histopathological scoring [21]. The histopathological hemispheric tissue volume atrophy analysis confirmed a prolonged neuroprotective efficacy of IAIPs in the young adult male + female rats after exposure of neonates to HI (Fig. 6). The reductions in the percent of hemispheric volume atrophy confirmed that IAIPs have durable neuroprotective effects in young adult rats even 35 days after exposure of the neonates to HI. However, the T_2 MRI imaging analysis was not able to identify significant IAIP-related beneficial effects between the study groups on P41 (Fig. 4). The discrepancy between the histopathological hemispheric volume atrophy measures and the MRI image analysis could be related to the fact that the hemispheric volume atrophy measures represent direct measures of the extent of overall injury to the whole brain, whereas the MRI measures depend upon indirect T_2 image analysis measures of discrete slices across the brain. Therefore, the potential greater sensitivity of the hemispheric tissue volume atrophy measures most likely accounts for our ability to detect the protective effect of treatment with IAIPs in the young adult rats. Nonetheless, our correlations between the T_2-weighted MRI and the histopathological hemispheric volume atrophy measures showed reasonable R^2 values, suggesting that both measures are satisfactorily able to detect the HI-related brain injury (Fig. 7). Taken together, our findings suggest that treatment with IAIPs attenuate HI-related brain injury as determined by MRI imaging early after injury but the effects of IAIPs were durable because their ability to attenuate the extent of the injury was still apparent in young adult rats.

Although we did not examine the mechanism(s) of action of the IAIPs in the current study including inhibition of destructive serine proteases or proinflammatory cytokines, previous work has shown that IAIPs protect the blood–brain barrier and downregulate circulating interleukin-6 in LPS-exposed mice [37] and block pro-inflammatory cytokines in sepsis in neonates and adults [31–33]. Consequently, it would be of interest to examine the ability of treatment with IAIPs to attenuate proinflammatory cytokines after exposure to HI in developing rats in future studies.

Accurate assessment of neurobehavioral outcomes is important because after exposure of neonates to brain injury, motor and cognitive deficits represent key sequelae in children [108, 109]. Many studies have utilized the Rice-Vannucci model of exposure to HI to examine neurodevelopmental outcomes after HI [20, 34, 35, 42, 110–113]. Systemic administration of IAIPs improved early motor coordination skills over time as measured by the righting reflex test in the males + females and in the male rats, whereas changes were not detected in the female rats (Fig. 8). A similar finding was previously reported in the same animal model because the administration of acetyl-L-carnitine improved righting reflex latencies after exposure to HI in males, but not in females [114]. Systemic treatment with IAIPs also improved early neuromuscular and locomotor function as determined by the wire hang test in the males + females and in the females and long-term spatial learning and memory determined by the Morris water maze test in the males + females and in the females (Fig. 10). However, we did not observe any effects of treatment with IAIPs on early general locomotive activity and exploratory behavior (small open field test). Similar findings have been reported, in which overall locomotive function was

not affected by HI injury in neonates [115, 116]. Therefore, the beneficial effects of treatment with IAIPs varied by sex for the different tests with the females appearing to benefit more in the tests performed later (Fig. 10). We have previously shown that IAIPs reduce neutrophil infiltration and microglia activation preferentially in male pups after exposure to HI [36]. Therefore, in the current study, we cannot rule out the possibility that the lack of effect on some of the behavioral outcomes selectively in the male pups could be due to the limited numbers of male pups or to the potential relatively lower amounts of IAIP suppression of neuroinflammation in the females compared with the males, thereby selectively resulting in improvements in behavioral outcomes in the females.

The extent to which the improvements in the behavioral outcomes could be attributed to the beneficial effects of IAIPs on brain weights, MRI changes, and decreases in the hemispheric tissue atrophy cannot be determined by the current study because the improvement in brain weight was observed in the males + females but not in either sex alone, the improvement in the MRI determinants was observed in the males + females and in females, and the improvement in hemispheric tissue atrophy was observed in the males + females but not in the individual sexes. Moreover, some of the differences with regard to the males + females could also relate to the larger number of animals examined when the sexes were combined.

Two different injury hemispheric atrophy patterns were observed after IAIP treatment particularly in the males. This is probably a result of the known variability in the Rice-Vannucci HI model [54, 117–119], the limited number of rat pups studied, and the different responses of the male and female pups to the treatment with IAIPs after exposure to neonatal HI. Therefore, a larger number of rat pups would be needed in order to reduce the variability in future studies. The mechanisms underlying the sex differences in response to treatment with IAIPs remain to be determined [21, 36, 38]. One possibility that could account for differential responses of the males and females could be different responses to HI as neonates [120]. However, sex-related differences from a neuropathological perspective have not been previously reported as the basis for sex-related differences in behavioral outcomes [120]. In the present study, we used our previous protocol to introduce a moderate severity of HI in the neonatal rats [21, 36]. We observed that the female neonatal rats benefited more from treatment with IAIPs with regard to relative improvement MRI detected edema/injury formation and later motor function. However, our findings differ somewhat from previous reports suggesting that female neonatal rats are often more resistant to injury compared with their male counterparts [120–122].

There are several limitations to our study and opportunities for future study. Although the pups were randomized as a block within each litter, we were not able to balance the groups by sex because there were more females than males born in some litters. Therefore, the numbers of males and females were not balanced in our study, which could have resulted in false-negative differences in some comparisons. Cresyl violet staining represents an estimate of neuronal loss and more specific immunohistochemical staining for studying mechanisms of actions of IAIPs using neuronal, astrocytic, microglia, and oligodendrocyte markers were not performed in the current study, especially at the different neurodevelopmental stages at which the behavioral tests were performed. However, we have previously shown that treatment with IAIPs reduces the effects of HI on these specific markers of brain injury in neonatal rats exposed to HI [21, 36]. In contrast to our previous studies, we administered 11 doses of IAIPs in an effort to facilitate exposure to IAIPs over the longer duration of the current studies [21, 36, 38]. However, we cannot be certain the increased number of doses had additional beneficial effects beyond or original treatment paradigm [21, 36, 38].

Conclusions

Systemic treatment with human blood-derived IAIPs provides short- and long-term protective effects on HI-related edema formation and evolution, attenuate hemispheric tissue loss, and neurobehavioral outcomes in rats after neonatal HI injury in a sex-dependent manner. Consequently, the findings of the current study, along with our former work [20, 21, 36, 38], can be interpreted to suggest that IAIPs could represent potentially important neuroprotective agents that could serve as alternative or adjunctive treatments to hypothermia.

Abbreviations CP: Cerebral palsy; HI: Hypoxic ischemia; HIE: Hypoxic-ischemic encephalopathy; IAIPs: Inter-alpha inhibitor proteins; LPS: Lipopolysaccharide; MRI: Magnetic resonance imaging

Supplementary Information The online version contains supplementary material available at https://doi.org/10.1007/s13311-022-01217-8.

Required Author Forms Disclosure forms provided by the authors are available with the online version of this article.

Funding Research reported in this publication was supported by the National Institute of General Medical Sciences (NIGMS) of the National Institutes of Health (NIH) under the following award numbers: Institutional Development Award (IDeA) from NIGMS under grant numbers 1R21-NS095130, 1R21-NS096525, R44-NS084575-02, 2R01HD057100, and R01-GM24211, the COBRE Center for Central Nervous System Function 1P20GM103645-01A1 and R35-131800, and an Emerging Areas of New Science Deans Award from Brown Biomed Division, Brown University. The authors assume all responsibility for the study and assert that the contents herein do not represent the official views of the NIH.

Declarations

Ethics Approval The experimental procedures in this study were performed after obtaining approval from the Institutional Animal Care and Use Committees (IACUC) of Brown University and Women & Infants Hospital of Rhode Island. All experimental procedures were carried out following the National Institutes of Health (NIH) guide for the care and use of laboratory animals.

Disclosures Y-P Lim is employed by ProThera Biologics, Inc. and has a significant financial stake in the company. All other authors declare that the submitted work was not carried out in the presence of any personal, professional, or financial relationships that could potentially be construed as a conflict of interest.

References

1. Vannucci RC. Hypoxic-ischemic encephalopathy. Am J Perinatol. 2000;17(3):113–20.
2. Stanley FJ. The aetiology of cerebral palsy. Early Hum Dev. 1994;36(2):81–8.
3. Mesterman R, Leitner Y, Yifat R, Gilutz G, Levi-Hakeini O, Bitchonsky O, et al. Cerebral palsy–long-term medical, functional, educational, and psychosocial outcomes. J Child Neurol. 2010;25(1):36–42.
4. Jan MM. Cerebral palsy: comprehensive review and update. Ann Saudi Med. 2006;26(2):123–32.
5. Klahr AC, Nadeau CA, Colbourne F. Temperature control in rodent neuroprotection studies: methods and challenges. Ther Hypothermia Temp Manag. 2017;7(1):42–9.
6. Cotten CM, Shankaran S. Hypothermia for hypoxic-ischemic encephalopathy. Expert Rev Obstet Gynecol. 2010;5(2):227–39.
7. Osredkar D, Thoresen M, Maes E, Flatebo T, Elstad M, Sabir H. Hypothermia is not neuroprotective after infection-sensitized neonatal hypoxic-ischemic brain injury. Resuscitation. 2014;85(4):567–72.
8. Gluckman PD, Gunn AJ, Wyatt JS. Hypothermia for neonates with hypoxic-ischemic encephalopathy. N Engl J Med. 2006;354(15):1643–5.
9. Gunn AJ, Gunn TR, de Haan HH, Williams CE, Gluckman PD. Dramatic neuronal rescue with prolonged selective head cooling after ischemia in fetal lambs. J Clin Invest. 1997;99(2):248–56.
10. Higgins RD, Raju TN, Perlman J, Azzopardi DV, Blackmon LR, Clark RH, et al. Hypothermia and perinatal asphyxia: executive summary of the National Institute of Child Health and Human Development workshop. J Pediatr. 2006;148(2):170–5.
11. Shankaran S, Laptook AR, Ehrenkranz RA, Tyson JE, McDonald SA, Donovan EF, et al. Whole-body hypothermia for neonates with hypoxic-ischemic encephalopathy. N Engl J Med. 2005;353(15):1574–84.
12. Shankaran S, Pappas A, McDonald SA, Vohr BR, Hintz SR, Yolton K, et al. Childhood outcomes after hypothermia for neonatal encephalopathy. N Engl J Med. 2012;366(22):2085–92.
13. Ferriero DM. Neonatal brain injury. N Engl J Med. 2004;351(19):1985–95.
14. Ten VS, Starkov A. Hypoxic-ischemic injury in the developing brain: the role of reactive oxygen species originating in mitochondria. Neurol Res Int. 2012;2012:542976.
15. Leonardo CC, Pennypacker KR. Neuroinflammation and MMPs: potential therapeutic targets in neonatal hypoxic-ischemic injury. J Neuroinflammation. 2009;6:13.
16. Bhalala US, Koehler RC, Kannan S. Neuroinflammation and neuroimmune dysregulation after acute hypoxic-ischemic injury of developing brain. Front Pediatr. 2014;2:144.
17. Carty ML, Wixey JA, Colditz PB, Buller KM. Post-insult minocycline treatment attenuates hypoxia-ischemia-induced neuroinflammation and white matter injury in the neonatal rat: a comparison of two different dose regimens. Int J Dev Neurosci. 2008;26(5):477–85.
18. Chew LJ, Takanohashi A, Bell M. Microglia and inflammation: impact on developmental brain injuries. Ment Retard Dev Disabil Res Rev. 2006;12(2):105–12.
19. Tang M, Alexander H, Clark RS, Kochanek PM, Kagan VE, Bayir H. Minocycline reduces neuronal death and attenuates microglial response after pediatric asphyxial cardiac arrest. J Cereb Blood Flow Metab. 2010;30(1):119–29.
20. Threlkeld SW, Gaudet CM, La Rue ME, Dugas E, Hill CA, Lim YP, et al. Effects of inter-alpha inhibitor proteins on neonatal brain injury: age, task and treatment dependent neurobehavioral outcomes. Exp Neurol. 2014;261:424–33.
21. Chen X, Nakada S, Donahue JE, Chen RH, Tucker R, Qiu J, et al. Neuroprotective effects of inter-alpha inhibitor proteins after hypoxic-ischemic brain injury in neonatal rats. Exp Neurol. 2019;317:244–59.
22. McCullough LD, Roy-O'Reilly M, Lai Y-J, Patrizz A, Xu Y, Lee J, et al. Exogenous inter-α inhibitor proteins prevent cell death and improve ischemic stroke outcomes in mice. J Clin Invest. 2021;131(17).
23. Zhu L, Zhuo L, Watanabe H, Kimata K. Equivalent involvement of inter-alpha-trypsin inhibitor heavy chain isoforms in forming covalent complexes with hyaluronan. Connect Tissue Res. 2008;49(1):48–55.
24. Potempa J, Kwon K, Chawla R, Travis J. Inter-alpha-trypsin inhibitor. Inhibition spectrum of native and derived forms. J Biol Chem. 1989;264(25):15109–14.
25. Yano T, Anraku S, Nakayama R, Ushijima K. Neuroprotective effect of urinary trypsin inhibitor against focal cerebral ischemia-reperfusion injury in rats. Anesthesiology. 2003;98(2):465–73.
26. Wang X, Xue Q, Yan F, Li L, Liu J, Li S, et al. Ulinastatin as a neuroprotective and anti-inflammatory agent in infant piglets model undergoing surgery on hypothermic low-flow cardiopulmonary bypass. Paediatr Anaesth. 2013;23(3):209–16.
27. Abe H, Sugino N, Matsuda T, Kanamaru T, Oyanagi S, Mori H. Effect of ulinastatin on delayed neuronal death in the gerbil hippocampus. Masui. 1996;45(1):38–43.
28. Shu Y, Yang Y, Qiu W, Lu Z, Li Y, Bao J, et al. Neuroprotection by ulinastatin in experimental autoimmune encephalomyelitis. Neurochem Res. 2011;36(11):1969–77.
29. Sjoberg EM, Blom A, Larsson BS, Alston-Smith J, Sjoquist M, Fries E. Plasma clearance of rat bikunin: evidence for receptor-mediated uptake. Biochem J. 1995;308(Pt 3):881–7.
30. Chen X, Song D, Nakada S, Qiu J, Iwamoto K, Chen RH, et al. Pharmacokinetics of inter-alpha inhibitor proteins and effects on hemostasis after hypoxic-ischemic brain injury in neonatal rats. Curr Pharm Des. 2020;26(32):3997–4006.
31. Yang S, Lim YP, Zhou M, Salvemini P, Schwinn H, Josic D, et al. Administration of human inter-alpha-inhibitors maintains hemodynamic stability and improves survival during sepsis. Crit Care Med. 2002;30(3):617–22.
32. Garantziotis S, Hollingsworth JW, Ghanayem RB, Timberlake S, Zhuo L, Kimata K, et al. Inter-alpha-trypsin inhibitor attenuates complement activation and complement-induced lung injury. J Immunol. 2007;179(6):4187–92.
33. Singh K, Zhang LX, Bendelja K, Heath R, Murphy S, Sharma S, et al. Inter-alpha inhibitor protein administration improves survival from neonatal sepsis in mice. Pediatr Res. 2010;68(3):242–7.
34. Gaudet CM, Lim YP, Stonestreet BS, Threlkeld SW. Effects of age, experience and inter-alpha inhibitor proteins on working

memory and neuronal plasticity after neonatal hypoxia-ischemia. Behav Brain Res. 2016;302:88–99.
35. Threlkeld SW, Lim YP, La Rue M, Gaudet C, Stonestreet BS. Immuno-modulator inter-alpha inhibitor proteins ameliorate complex auditory processing deficits in rats with neonatal hypoxic-ischemic brain injury. Brain Behav Immun. 2017;64:173–9.
36. Barrios-Anderson A, Chen X, Nakada S, Chen R, Lim YP, Stonestreet BS. Inter-alpha inhibitor proteins modulate neuroinflammatory biomarkers after hypoxia-ischemia in neonatal rats. J Neuropathol Exp Neurol. 2019.
37. Logsdon AF, Erickson MA, Chen X, Qiu J, Lim YP, Stonestreet BS, et al. Inter-alpha inhibitor proteins attenuate lipopolysaccharide-induced blood-brain barrier disruption and downregulate circulating interleukin 6 in mice. J Cereb Blood Flow Metab. 2020;40(5):1090–102.
38. Schuffels S, Nakada S, Wu Y, Lim YP, Chen X, Stonestreet BS. Effects of inter-alpha inhibitor proteins on brain injury after exposure of neonatal rats to severe hypoxia-ischemia. Exp Neurol. 2020;334:113442.
39. Semple BD, Blomgren K, Gimlin K, Ferriero DM, Noble-Haeusslein LJ. Brain development in rodents and humans: identifying benchmarks of maturation and vulnerability to injury across species. Prog Neurobiol. 2013;106–107:1–16.
40. McCutcheon JE, Marinelli M. Age matters. Eur J Neurosci. 2009;29(5):997–1014.
41. Cai Y, Liu S, Li N, Xu S, Zhang Y, Chan P. Postnatal ontogenesis of molecular clock in mouse striatum. Brain Res. 2009;1264:33–8.
42. Penny TR, Pham Y, Sutherland AE, Smith MJ, Lee J, Jenkin G, et al. Optimization of behavioral testing in a long-term rat model of hypoxic ischemic brain injury. Behav Brain Res. 2021;409:113322.
43. Hassell KJ, Ezzati M, Alonso-Alconada D, Hausenloy DJ, Robertson NJ. New horizons for newborn brain protection: enhancing endogenous neuroprotection. Arch Dis Child Fetal Neonatal Ed. 2015;100(6):F541–52.
44. Cowan WM. The development of the brain. Sci Am. 1979;241(3):113–33.
45. Dobbing J, Sands J. Comparative aspects of the brain growth spurt. Early Hum Dev. 1979;3(1):79–83.
46. Sawada M, Alkayed NJ, Goto S, Crain BJ, Traystman RJ, Shaivitz A, et al. Estrogen receptor antagonist ICI182,780 exacerbates ischemic injury in female mouse. J Cereb Blood Flow Metab. 2000;20(1):112–8.
47. Terao S, Yilmaz G, Stokes KY, Ishikawa M, Kawase T, Granger DN. Inflammatory and injury responses to ischemic stroke in obese mice. Stroke. 2008;39(3):943–50.
48. Lim YP. ProThera Biologics Inc.: a novel immunomodulator and biomarker for life-threatening diseases. R I Med J. 2013;96(2):16–8.
49. Opal SM, Lim YP, Cristofaro P, Artenstein AW, Kessimian N, Delsesto D, et al. Inter-alpha inhibitor proteins: a novel therapeutic strategy for experimental anthrax infection. Shock. 2011;35(1):42–4.
50. Spasova MS, Sadowska GB, Threlkeld SW, Lim YP, Stonestreet BS. Ontogeny of inter-alpha inhibitor proteins in ovine brain and somatic tissues. Exp Biol Med (Maywood). 2014;239(6):724–36.
51. Lim YP, Josic D, Callanan H, Brown J, Hixson DC. Affinity purification and enzymatic cleavage of inter-alpha inhibitor proteins using antibody and elastase immobilized on CIM monolithic disks. J Chromatogr A. 2005;1065(1):39–43.
52. Rice JE 3rd, Vannucci RC, Brierley JB. The influence of immaturity on hypoxic-ischemic brain damage in the rat. Ann Neurol. 1981;9(2):131–41.
53. Chen X, Zhang J, Kim B, Jaitpal S, Meng SS, Adjepong K, et al. High-mobility group box-1 translocation and release after hypoxic ischemic brain injury in neonatal rats. Exp Neurol. 2019;311:1–14.
54. Towfighi J, Mauger D, Vannucci RC, Vannucci SJ. Influence of age on the cerebral lesions in an immature rat model of cerebral hypoxia-ischemia: a light microscopic study. Brain Res Dev Brain Res. 1997;100(2):149–60.
55. Thoresen M, Hobbs CE, Wood T, Chakkarapani E, Dingley J. Cooling combined with immediate or delayed xenon inhalation provides equivalent long-term neuroprotection after neonatal hypoxia-ischemia. J Cereb Blood Flow Metab. 2009;29(4):707–14.
56. Dingley J, Tooley J, Porter H, Thoresen M. Xenon provides short-term neuroprotection in neonatal rats when administered after hypoxia-ischemia. Stroke. 2006;37(2):501–6.
57. Thoresen M, Bagenholm R, Loberg EM, Apricena F, Kjellmer I. Posthypoxic cooling of neonatal rats provides protection against brain injury. Arch Dis Child Fetal Neonatal Ed. 1996;74(1):F3-9.
58. Thoresen M, Bagenholm R, Loberg EM, Apriccna F. The stress of being restrained reduces brain damage after a hypoxic-ischaemic insult in the 7-day-old rat. NeuroReport. 1996;7(2):481–4.
59. Bona E, Hagberg H, Loberg EM, Bagenholm R, Thoresen M. Protective effects of moderate hypothermia after neonatal hypoxia-ischemia: short- and long-term outcome. Pediatr Res. 1998;43(6):738–45.
60. Ma D, Hossain M, Chow A, Arshad M, Battson RM, Sanders RD, et al. Xenon and hypothermia combine to provide neuroprotection from neonatal asphyxia. Ann Neurol. 2005;58(2):182–93.
61. Cho KH, Davidson JO, Dean JM, Bennet L, Gunn AJ. Cooling and immunomodulation for treating hypoxic-ischemic brain injury. Pediatr Int. 2020;62(7):770–8.
62. Lear BA, Lear CA, Davidson JO, Sae-Jiw J, Lloyd JM, Gunn AJ, et al. Tertiary cystic white matter injury as a potential phenomenon after hypoxia-ischaemia in preterm f sheep. Brain Commun. 2021;3(2):fcab024.
63. Lin CY, Chang YC, Wang ST, Lee TY, Lin CF, Huang CC. Altered inflammatory responses in preterm children with cerebral palsy. Ann Neurol. 2010;68(2):204–12.
64. Wassink G, Davidson JO, Fraser M, Yuill CA, Bennet L, Gunn AJ. Non-additive effects of adjunct erythropoietin therapy with therapeutic hypothermia after global cerebral ischaemia in near-term fetal sheep. J Physiol. 2020;598(5):999–1015.
65. Zhou KQ, Davidson JO, Bennet L, Gunn AJ. Combination treatments with therapeutic hypothermia for hypoxic-ischemic neuroprotection. Dev Med Child Neurol. 2020;62(10):1131–7.
66. Zhang L, Nair A, Krady K, Corpe C, Bonneau RH, Simpson IA, et al. Estrogen stimulates microglia and brain recovery from hypoxia-ischemia in normoglycemic but not diabetic female mice. J Clin Invest. 2004;113(1):85–95.
67. Ellingson BM, Cloughesy TF, Lai A, Nghiemphu PL, Lalezari S, Zaw T, et al. Quantification of edema reduction using differential quantitative T2 (DQT2) relaxometry mapping in recurrent glioblastoma treated with bevacizumab. J Neurooncol. 2012;106(1):111–9.
68. Brant-Zawadzki M, Bartkowski HM, Ortendahl DA, Pitts LH, Hylton NM, Nishimura MC, et al. NMR in experimental cerebral edema: value of T1 and T2 calculations. AJNR Am J Neuroradiol. 1984;5(2):125–9.
69. Kato H, Kogure K, Ohtomo H, Izumiyama M, Tobita M, Matsui S, et al. Characterization of experimental ischemic brain edema utilizing proton nuclear magnetic resonance imaging. J Cereb Blood Flow Metab. 1986;6(2):212–21.
70. Naruse S, Horikawa Y, Tanaka C, Hirakawa K, Nishikawa H, Yoshizaki K. Proton nuclear magnetic resonance studies on brain edema. J Neurosurg. 1982;56(6):747–52.
71. Li J, Benashski SE, Venna VR, McCullough LD. Effects of metformin in experimental stroke. Stroke. 2010;41(11):2645–52.

72. Swanson RA, Morton MT, Tsao-Wu G, Savalos RA, Davidson C, Sharp FR. A semiautomated method for measuring brain infarct volume. J Cereb Blood Flow Metab. 1990;10(2):290–3.
73. Duan TT, Tan JW, Yuan Q, Cao J, Zhou QX, Xu L. Acute ketamine induces hippocampal synaptic depression and spatial memory impairment through dopamine D1/D5 receptors. Psychopharmacology. 2013;228(3):451–61.
74. Morris RG, Garrud P, Rawlins JN, O'Keefe J. Place navigation impaired in rats with hippocampal lesions. Nature. 1982;297(5868):681–3.
75. Grubbs F. Procedures for detecting outlying observations in samples. Technometrics. 1968;11(1):1–21.
76. Stefansky W. Rejecting outliers in factorial designs. Technometrics. 1972;14:469–79.
77. Motulsky HJ, Brown RE. Detecting outliers when fitting data with nonlinear regression - a new method based on robust nonlinear regression and the false discovery rate. BMC Bioinformatics. 2006;7:123.
78. Jahn-Eimermacher A, Lasarzik I, Raber J. Statistical analysis of latency outcomes in behavioral experiments. Behav Brain Res. 2011;221(1):271–5.
79. Trivedi R, Rathore R, Gupta R. Review: clinical application of diffusion tensor imaging. Indian J Radiol Imaging. 2008;18.
80. Brown RW Cheng YCN, Haacke EM, Thompson MR, Venkatesan RV. Magnetic resonance imaging - physical principles and sequence design, Chapter 4, p59: Wiley-Blackwell; 2nd Edition 2014.
81. Schreglmann M, Ground A, Vollmer B, Johnson MJ. Systematic review: long-term cognitive and behavioural outcomes of neonatal hypoxic-ischaemic encephalopathy in children without cerebral palsy. Acta Paediatr. 2020;109(1):20–30.
82. Silachev DN, Plotnikov EY, Pevzner IB, Zorova LD, Balakireva AV, Gulyaev MV, et al. Neuroprotective effects of mitochondria-targeted plastoquinone in a rat model of neonatal hypoxic(-)ischemic brain injury. Molecules. 2018;23(8).
83. Ten VS, Wu EX, Tang H, Bradley-Moore M, Fedarau MV, Ratner VI, et al. Late measures of brain injury after neonatal hypoxia-ischemia in mice. Stroke. 2004;35(9):2183–8.
84. Balduini W, De Angelis V, Mazzoni E, Cimino M. Simvastatin protects against long-lasting behavioral and morphological consequences of neonatal hypoxic/ischemic brain injury. Stroke. 2001;32(9):2185–91.
85. Fan LW, Lin S, Pang Y, Lei M, Zhang F, Rhodes PG, et al. Hypoxia-ischemia induced neurological dysfunction and brain injury in the neonatal rat. Behav Brain Res. 2005;165(1):80–90.
86. Lubics A, Reglodi D, Tamas A, Kiss P, Szalai M, Szalontay L, et al. Neurological reflexes and early motor behavior in rats subjected to neonatal hypoxic-ischemic injury. Behav Brain Res. 2005;157(1):157–65.
87. Muntsant A, Shrivastava K, Recasens M, Gimenez-Llort L. Severe perinatal hypoxic-ischemic brain injury induces long-term sensorimotor deficits, anxiety-like behaviors and cognitive impairment in a sex-, age- and task-selective manner in C57BL/6 mice but can be modulated by neonatal handling. Front Behav Neurosci. 2019;13:7.
88. Andine P, Thordstein M, Kjellmer I, Nordborg C, Thiringer K, Wennberg E, et al. Evaluation of brain damage in a rat model of neonatal hypoxic-ischemia. J Neurosci Methods. 1990;35(3):253–60.
89. Cabaj A, Bekiesinska-Figatowska M, Madzik J. MRI patterns of hypoxic-ischemic brain injury in preterm and full term infants - classical and less common MR findings. Pol J Radiol. 2012;77(3):71–6.
90. Doman SE, Girish A, Nemeth CL, Drummond GT, Carr P, Garcia MS, et al. Early detection of hypothermic neuroprotection using T2-weighted magnetic resonance imaging in a mouse model of hypoxic ischemic encephalopathy. Front Neurol. 2018;9:304.
91. Aggarwal M, Burnsed J, Martin LJ, Northington FJ, Zhang J. Imaging neurodegeneration in the mouse hippocampus after neonatal hypoxia-ischemia using oscillating gradient diffusion MRI. Magn Reson Med. 2014;72(3):829–40.
92. Xu J, Zou Y, Zhang LH, Wai MS, Kung HF, Ge ZY, et al. Postmortem MRI changes of the brains of the rats of different ages. Int J Neurosci. 2008;118(7):1039–50.
93. Barkovich AJ. Concepts of myelin and myelination in neuroradiology. AJNR Am J Neuroradiol. 2000;21(6):1099–109.
94. Prayer D, Prayer L. Diffusion-weighted magnetic resonance imaging of cerebral white matter development. Eur J Radiol. 2003;45(3):235–43.
95. Matsumae M, Kurita D, Atsumi H, Haida M, Sato O, Tsugane R. Sequential changes in MR water proton relaxation time detect the process of rat brain myelination during maturation. Mech Ageing Dev. 2001;122(12):1281–91.
96. Barkovich AJ, Kjos BO, Jackson DE Jr, Norman D. Normal maturation of the neonatal and infant brain: MR imaging at 1.5 T. Radiology. 1988;166(1 Pt 1):173–80.
97. Kucharczyk W, Macdonald PM, Stanisz GJ, Henkelman RM. Relaxivity and magnetization transfer of white matter lipids at MR imaging: importance of cerebrosides and pH. Radiology. 1994;192(2):521–9.
98. Baumann N, Pham-Dinh D. Biology of oligodendrocyte and myelin in the mammalian central nervous system. Physiol Rev. 2001;81(2):871–927.
99. Poduslo SE, Jang Y. Myelin development in infant brain. Neurochem Res. 1984;9(11):1615–26.
100. Aden U, Dahlberg V, Fredholm BB, Lai LJ, Chen Z, Bjelke B. MRI evaluation and functional assessment of brain injury after hypoxic ischemia in neonatal mice. Stroke. 2002;33(5):1405–10.
101. Dubois J, Dehaene-Lambertz G, Kulikova S, Poupon C, Huppi PS, Hertz-Pannier L. The early development of brain white matter: a review of imaging studies in fetuses, newborns and infants. Neuroscience. 2014;276:48–71.
102. Wang S, Ledig C, Hajnal JV, Counsell SJ, Schnabel JA, Deprez M. Quantitative assessment of myelination patterns in preterm neonates using T2-weighted MRI. Sci Rep. 2019;9(1):12938.
103. Tuor UI, Kozlowski P, Del Bigio MR, Ramjiawan B, Su S, Malisza K, et al. Diffusion- and T2-weighted increases in magnetic resonance images of immature brain during hypoxia-ischemia: transient reversal posthypoxia. Exp Neurol. 1998;150(2):321–8.
104. Fau S, Po C, Goyenvalle C, Meric P, Charriaut-Marlangue C. Do early MRI signals predict lesion size in a neonatal stroke rat model?. AJNR Am J Neuroradiol. 2013;34(7):E73–6.
105. Lodygensky GA, West T, Moravec MD, Back SA, Dikranian K, Holtzman DM, et al. Diffusion characteristics associated with neuronal injury and glial activation following hypoxia-ischemia in the immature brain. Magn Reson Med. 2011;66(3):839–45.
106. Wang Y, Cheung PT, Shen GX, Wu EX, Cao G, Bart I, et al. Hypoxic-ischemic brain injury in the neonatal rat model: relationship between lesion size at early MR imaging and irreversible infarction. AJNR Am J Neuroradiol. 2006;27(1):51–4.
107. Lou M, Eschenfelder CC, Herdegen T, Brecht S, Deuschl G. Therapeutic window for use of hyperbaric oxygenation in focal transient ischemia in rats. Stroke. 2004;35(2):578–83.
108. Knox-Concepcion KR, Figueroa JD, Hartman RE, Li Y, Zhang L. Repression of the glucocorticoid receptor increases hypoxic-ischemic brain injury in the male neonatal rat. Int J Mol Sci. 2019;20(14).
109. Coleman MB, Glass P, Brown J, Kadom N, Tsuchida T, Scafidi J, et al. Neonatal neurobehavioral abnormalities and MRI brain injury in encephalopathic newborns treated with hypothermia. Early Hum Dev. 2013;89(9):733–7.
110. McDonald CA, Penny TR, Paton MCB, Sutherland AE, Nekkanti L, Yawno T, et al. Effects of umbilical cord blood cells, and subtypes,

to reduce neuroinflammation following perinatal hypoxic-ischemic brain injury. J Neuroinflammation. 2018;15(1):47.
111. Tanaka E, Ogawa Y, Mukai T, Sato Y, Hamazaki T, Nagamura-Inoue T, et al. Dose-dependent effect of intravenous administration of human umbilical cord-derived mesenchymal stem cells in neonatal stroke mice. Front Neurol. 2018;9:133.
112. Pimentel-Coelho PM, Magalhaes ES, Lopes LM, deAzevedo LC, Santiago MF, Mendez-Otero R. Human cord blood transplantation in a neonatal rat model of hypoxic-ischemic brain damage: functional outcome related to neuroprotection in the striatum. Stem Cells Dev. 2010;19(3):351–8.
113. Bradford A, Hernandez M, Kearney E, Theriault L, Lim YP, Stonestreet BS, et al. Effects of juvenile or adolescent working memory experience and inter-alpha inhibitor protein treatment after neonatal hypoxia-ischemia. Brain Sci. 2020;10(12).
114. Tang S, Xu S, Lu X, Gullapalli RP, McKenna MC, Waddell J. Neuroprotective effects of acetyl-L-carnitine on neonatal hypoxia ischemia-induced brain injury in rats. Dev Neurosci. 2016;38(5):384–96.
115. Arteaga O, Revuelta M, Uriguen L, Martinez-Millan L, Hilario E, Alvarez A. Docosahexaenoic acid reduces cerebral damage and ameliorates long-term cognitive impairments caused by neonatal hypoxia-ischemia in rats. Mol Neurobiol. 2017;54(9):7137–55.
116. Moran J, Stokowska A, Walker FR, Mallard C, Hagberg H, Pekna M. Intranasal C3a treatment ameliorates cognitive impairment in a mouse model of neonatal hypoxic-ischemic brain injury. Exp Neurol. 2017;290:74–84.
117. Failor S, Nguyen V, Darcy DP, Cang J, Wendland MF, Stryker MP, et al. Neonatal cerebral hypoxia-ischemia impairs plasticity in rat visual cortex. J Neurosci. 2010;30(1):81–92.
118. McQuillen PS, Ferriero DM. Selective vulnerability in the developing central nervous system. Pediatr Neurol. 2004;30(4):227–35.
119. Sabir H, Scull-Brown E, Liu X, Thoresen M. Immediate hypothermia is not neuroprotective after severe hypoxia-ischemia and is deleterious when delayed by 12 hours in neonatal rats. Stroke. 2012;43(12):3364–70.
120. Smith AL, Alexander M, Rosenkrantz TS, Sadek ML, Fitch RH. Sex differences in behavioral outcome following neonatal hypoxia ischemia: insights from a clinical meta-analysis and a rodent model of induced hypoxic ischemic brain injury. Exp Neurol. 2014;254:54–67.
121. Cohen SS, Stonestreet BS. Sex differences in behavioral outcome following neonatal hypoxia ischemia: insights from a clinical meta-analysis and a rodent model of induced hypoxic ischemic injury. Exp Neurol. 2014;256:70–3.
122. Hill CA, Fitch RH. Sex differences in mechanisms and outcome of neonatal hypoxia-ischemia in rodent models: implications for sex-specific neuroprotection in clinical neonatal practice. Neurol Res Int. 2012;2012:867531.